SIAM J. NUMER. ANAL.
Vol. 44, No. 5, pp. 2082–2106

A MULTIPOINT FLUX MIXED FINITE ELEMENT METHOD*

MARY F. WHEELER† AND IVAN YOTOV‡

Abstract. We develop a mixed finite element method for single phase flow in porous media that reduces to cell-centered finite differences on quadrilateral and simplicial grids and performs well for discontinuous full tensor coefficients. Motivated by the multipoint flux approximation method where subedge fluxes are introduced, we consider the lowest order Brezzi–Douglas–Marini (BDM) mixed finite element method. A special quadrature rule is employed that allows for local velocity elimination and leads to a symmetric and positive definite cell-centered system for the pressures. Theoretical and numerical results indicate second-order convergence for pressures at the cell centers and first-order convergence for subedge fluxes. Second-order convergence for edge fluxes is also observed computationally if the grids are sufficiently regular.

Key words. mixed finite element, multipoint flux approximation, cell-centered finite difference, tensor coefficient, error estimates

AMS subject classifications. 65N06, 65N12, 65N15, 65N30, 76S05

DOI. 10.1137/050638473

1. Introduction.

Mixed finite element (MFE) methods have been widely used for modeling flow in porous media due to their local mass conservation, accurate approximation of the velocity, and proper treatment of discontinuous coefficients. A computational drawback of these methods is the need to solve an algebraic system of saddle point type. One possible approach to address this issue is to use the hybrid form of the MFE method [9, 15]. In this case the method can be reduced to a symmetric positive definite system for the pressure Lagrange multipliers on the element faces. Alternatively, it was established in [29] that, in the case of diagonal tensor coefficients and rectangular grids, MFE methods can be reduced to cell-centered finite differences (CCFD) for the pressure through the use of a quadrature rule for the velocity mass matrix. This relationship was explored in [33] to obtain convergence of CCFD on rectangular grids. This result was extended to full tensor coefficients and logically rectangular grids in [7, 6], where the expanded mixed finite element (EMFE) method was introduced. The EMFE method is very accurate for smooth grids and coefficients, but loses accuracy near discontinuities. This is due to the arithmetic averaging of discontinuous coefficients. Higher order accuracy can be recovered if pressure Lagrange multipliers are introduced along discontinuous interfaces [6], but then the cell-centered structure is lost.

Several other methods have been introduced that handle well rough grids and coefficients. The control volume mixed finite element (CVMFE) method [16] is based on discretizing Darcy's law on specially constructed control volumes. Mimetic finite difference (MFD) methods [23] are designed to mimic on the discrete level critical

*Received by the editors August 19, 2005; accepted for publication (in revised form) April 6, 2006; published electronically October 30, 2006.
http://www.siam.org/journals/sinum/44-5/63847.html

†Institute for Computational Engineering and Sciences (ICES), Department of Aerospace Engineering & Engineering Mechanics and Department of Petroleum and Geosystems Engineering, The University of Texas at Austin, Austin, TX 78712 (mfw@ices.utexas.edu). The research of this author was partially supported by NSF grant DMS 0411413 and DOE grant DE-FGO2-04ER25617.

‡Department of Mathematics, University of Pittsburgh, Pittsburgh, PA 15260 (yotov@math.pitt.edu). The research of this author was supported in part by DOE grant DE-FG02-04ER25618 and NSF grant DMS 0411694.

properties of the differential operators. The approximating spaces in both methods are closely related to RT_0, the lowest order Raviart–Thomas MFE spaces [27]. These relationships have been explored in [17, 30] and [10, 12] to establish convergence of the CVMFE methods and the MFD methods, respectively. However, as in the case of MFE methods, both methods lead to an algebraic saddle point problem. The multipoint flux approximation (MPFA) method [1, 2, 19, 20] has been developed as a finite volume method and combines the advantages of the above mentioned methods; i.e., it is accurate for rough grids and coefficients and reduces to a cell-centered stencil for the pressures. However, due to the nonvariational formulation of the MPFA, there exist only limited theoretical results in the literature for the well posedness and convergence of this method [24].

In this paper we design a MFE method that reduces to accurate CCFD for full tensors and irregular grids and performs well for discontinuous coefficients. Motivated by the MPFA [2, 20], where subedge fluxes are introduced, we consider the lowest order Brezzi–Douglas–Marini (BDM) MFE method [14, 15]. In two dimensions, for example, there are two velocity degrees of freedom per edge. A special quadrature rule is employed that allows for local velocity elimination and leads to a cell-centered stencil for the pressures. The resulting algebraic system is symmetric and positive definite. We call our method a multipoint flux mixed finite element (MFMFE) method, due to its close relationship with the MPFA method.

We emphasize that the formulation of the MFMFE method involves K^{-1}; see (2.41)–(2.42). For diagonal discontinuous K, the resulting coefficient is a harmonic average. This explains the superior performance of the MFMFE method for problems with rough grids and coefficients, compared to the EMFE method.

The MFMFE method results in a smaller algebraic system than the hybrid MFE method does, since finite element partitions have fewer elements than edges or faces. Moreover, many existing petroleum simulators are based on cell-centered discretizations and their data structures are more compatible with the MFMFE method than with the hybrid MFE method.

The variational framework allows for MFE analysis tools to be combined with quadrature error analysis to establish well posedness and accuracy of the MFMFE method. We formulate and analyze the method on simplicial grids in two and three dimensions as well as on quadrilateral grids. We obtain first order convergence for the pressure in the L^2-norm and for the velocity in the $H(\mathrm{div})$-norm. A duality argument is employed to establish second order convergence for the pressure in a discrete L^2-norm involving the centers of mass of the elements.

The analysis in the quadrilateral case is more involved, since it requires mapping to a reference element. As a result a restriction needs to be imposed on the geometry of each quadrilateral, namely, that it is an $O(h^2)$-perturbation of a parallelogram; see (3.1). We have verified numerically that this restriction is not just an artifact of the analysis, but is needed in practice as well. We also note that second order convergence is observed numerically for the velocities at the midpoints of the edges on h^2-parallelogram grids.

The techniques used in this paper can be employed to formulate and analyze extensions of the MFMFE method to nonmatching multiblock grids via mortar finite elements in the spirit of [5], multiscale MFMFE methods in the spirit of [4], and adaptive mortar MFMFE methods in the spirit of [34].

The rest of the paper is organized as follows. The method is developed in section 2. Sections 3 and 4 are devoted to the error analysis of the velocity and the pressure, respectively. Numerical experiments are presented in section 5. We end with some conclusions in section 6.

2. Definition of the method.

2.1. Preliminaries. We consider the second order elliptic problem written as a system of two first order equations,

$$\mathbf{u} = -K\nabla p \quad \text{in } \Omega, \tag{2.1}$$
$$\nabla\cdot\mathbf{u} = f \quad \text{in } \Omega, \tag{2.2}$$
$$p = g \quad \text{on } \Gamma_D, \tag{2.3}$$
$$\mathbf{u}\cdot\mathbf{n} = 0 \quad \text{on } \Gamma_N, \tag{2.4}$$

where the domain $\Omega \subset \mathbf{R}^d$, $d = 2$ or 3, has a boundary $\partial\Omega = \overline{\Gamma}_D \cup \overline{\Gamma}_N$, $\Gamma_D \cap \Gamma_N = \emptyset$, measure$(\Gamma_D) > 0$, $\mathbf{n}$ is the outward unit normal on $\partial\Omega$, and K is a symmetric, uniformly positive definite tensor satisfying, for some $0 < k_0 \le k_1 < \infty$,

$$k_0\xi^T\xi \le \xi^T K(\mathbf{x})\xi \le k_1\xi^T\xi \quad \forall\mathbf{x}\in\Omega\ \forall\xi\in\mathbf{R}^d. \tag{2.5}$$

In flow in porous media modeling, p is the pressure, $\mathbf{u}$ is the Darcy velocity, and K represents the permeability divided by the viscosity. The choice of boundary conditions is made for the sake of simplicity. More general boundary conditions, including nonhomogeneous full Neumann problems, can also be treated.

Throughout this paper, C denotes a generic positive constant that is independent of the discretization parameter h. We will also use the following standard notation. For a domain $G \subset \mathbf{R}^d$, the $L^2(G)$ inner product and norm for scalar and vector valued functions are denoted $(\cdot,\cdot)_G$ and $\|\cdot\|_G$, respectively. The norms and seminorms of the Sobolev spaces $W^{k,p}(G)$, $k \in \mathbf{R}$, $p > 0$ are denoted by $\|\cdot\|_{k,p,G}$ and $|\cdot|_{k,p,G}$, respectively. The norms and seminorms of the Hilbert spaces $H^k(G)$ are denoted by $\|\cdot\|_{k,G}$ and $|\cdot|_{k,G}$, respectively. We omit G in the subscript if $G = \Omega$. For a section of the domain or element boundary $S \subset \mathbf{R}^{d-1}$ we write $\langle\cdot,\cdot\rangle_S$ and $\|\cdot\|_S$ for the $L^2(S)$ inner product (or duality pairing) and norm, respectively. For a tensor-valued function M, let $\|M\|_\alpha = \max_{i,j}\|M_{ij}\|_\alpha$ for any norm $\|\cdot\|_\alpha$. We will also use the space

$$H(\mathrm{div};\Omega) = \{\mathbf{v}\in(L^2(\Omega))^d : \nabla\cdot\mathbf{v}\in L^2(\Omega)\}$$

equipped with the norm

$$\|\mathbf{v}\|_{\mathrm{div}} = (\|\mathbf{v}\|^2 + \|\nabla\cdot\mathbf{v}\|^2)^{1/2}.$$

The weak formulation of (2.1)–(2.4) is the following: find $\mathbf{u}\in\mathbf{V}$ and $p \in W$ such that

$$(K^{-1}\mathbf{u},\mathbf{v}) = (p,\nabla\cdot\mathbf{v}) - \langle g,\mathbf{v}\cdot\mathbf{n}\rangle_{\Gamma_D}, \quad \mathbf{v}\in\mathbf{V}, \tag{2.6}$$
$$(\nabla\cdot\mathbf{u}, w) = (f, w), \quad w\in W, \tag{2.7}$$

where

$$\mathbf{V} = \{\mathbf{v}\in H(\mathrm{div};\Omega) : \mathbf{v}\cdot\mathbf{n} = 0 \text{ on } \Gamma_N\}, \quad W = L^2(\Omega).$$

It is well known [15, 28] that (2.6)–(2.7) has a unique solution.

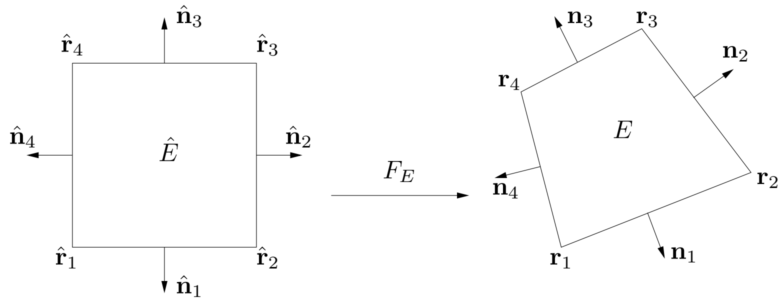

FIG. 2.1. *Mapping in the case of a quadrilateral.*

2.2. Finite element mappings. Consider a polygonal domain $\Omega \in \mathbf{R}^d$ and let $\mathcal{T}_h$ be a finite element partition of Ω consisting of triangles and/or convex quadrilaterals in two dimensions and tetrahedra in three dimensions, where $h = \max_{E\in\mathcal{T}_h} \operatorname{diam}(E)$. We assume that $\mathcal{T}_h$ is shape regular and quasi-uniform [18]. For any element $E \in \mathcal{T}_h$ there exists a bijection mapping $F_E : \hat{E} \to E$ where $\hat{E}$ is the reference element. Denote the Jacobian matrix by DF_E and let $J_E = |\det(DF_E)|$. Denote the inverse mapping by F_E^{-1}, its Jacobian matrix by DF_E^{-1}, and let $J_{F_E^{-1}} = |\det(DF_E^{-1})|$. We have that

$$DF_E^{-1}(x) = (DF_E)^{-1}(\hat{x}), \qquad J_{F_E^{-1}}(x) = \frac{1}{J_E(\hat{x})}.$$

In the case of convex quadrilaterals, $\hat{E}$ is the unit square with vertices $\hat{\mathbf{r}}_1 = (0,\, 0)^T$, $\hat{\mathbf{r}}_2 = (1,\, 0)^T$, $\hat{\mathbf{r}}_3 = (1,\, 1)^T$, and $\hat{\mathbf{r}}_4 = (0,\, 1)^T$. Denote by $\mathbf{r}_i = (x_i,\, y_i)^T$, $i = 1, \dots, 4$, the four corresponding vertices of element E as shown in Figure 2.1. The outward unit normal vectors to the edges of E and $\hat{E}$ are denoted by $\mathbf{n}_i$ and $\hat{\mathbf{n}}_i$, $i = 1, \dots, 4$, respectively. In this case F_E is the bilinear mapping given by

$$\begin{aligned} F_E(\hat{\mathbf{r}}) &= \mathbf{r}_1 (1-\hat{x})(1-\hat{y}) + \mathbf{r}_2\, \hat{x}(1-\hat{y}) + \mathbf{r}_3\, \hat{x}\hat{y} + \mathbf{r}_4\, (1-\hat{x})\hat{y} \\ &= \mathbf{r}_1 + \mathbf{r}_{21}\hat{x} + \mathbf{r}_{41}\hat{y} + (\mathbf{r}_{34} - \mathbf{r}_{21})\hat{x}\hat{y}, \end{aligned} \tag{2.8}$$

where $\mathbf{r}_{ij} = \mathbf{r}_i - \mathbf{r}_j$. It is easy to see that DF_E and J_E are linear functions of $\hat{x}$ and $\hat{y}$:

$$\begin{aligned} DF_E &= [(1-\hat{y})\, \mathbf{r}_{21} + \hat{y}\, \mathbf{r}_{34},\ (1-\hat{x})\, \mathbf{r}_{41} + \hat{x}\, \mathbf{r}_{32}] \\ &= [\mathbf{r}_{21}, \mathbf{r}_{41}] + [(\mathbf{r}_{34} - \mathbf{r}_{21})\hat{y}, (\mathbf{r}_{34} - \mathbf{r}_{21})\hat{x}], \end{aligned} \tag{2.9}$$

$$J_E = 2|T_1| + 2(|T_2| - |T_1|)\hat{x} + 2(|T_4| - |T_1|)\hat{y}, \tag{2.10}$$

where $|T_i|$ is the area of the triangle formed by the two edges sharing $\mathbf{r}_i$. Since E is convex, the Jacobian determinant J_E is uniformly positive, i.e., $J_E(\hat{x}, \hat{y}) > 0$.

In the case of triangles, $\hat{E}$ is the reference right triangle with vertices $\hat{\mathbf{r}}_1 = (0,\, 0)^T$, $\hat{\mathbf{r}}_2 = (1,\, 0)^T$, and $\hat{\mathbf{r}}_3 = (0,\, 1)^T$. Let $\mathbf{r}_1$, $\mathbf{r}_2$, and $\mathbf{r}_3$ be the corresponding vertices of E, oriented in a counterclockwise direction. The linear mapping for triangles has the form

$$F_E(\hat{\mathbf{r}}) = \mathbf{r}_1(1 - \hat{x} - \hat{y}) + \mathbf{r}_2\hat{x} + \mathbf{r}_3\hat{y}, \tag{2.11}$$

with respective Jacobian matrix and Jacobian determinant

$$DF_E = [\mathbf{r}_{21}, \mathbf{r}_{31}]^T \quad \text{and} \quad J_E = 2|E|. \tag{2.12}$$

The mapping in the case of tetrahedra is described similarly to the triangular case. Note that in the case of simplicial elements the mapping is affine and the Jacobian matrix and its determinant are constants.

Using the mapping definitions (2.8)–(2.12), it is easy to check that for any edge (face) $e_i \subset \partial E$

$$\mathbf{n}_i = \frac{1}{|e_i|} J_E (DF_E^{-1})^T \hat{\mathbf{n}}_i. \tag{2.13}$$

It is also easy to see that, for all element types, the mapping definitions and the shape-regularity and quasiuniformity of the grids imply that

$$\|DF_E\|_{0,\infty,\hat{E}} \sim h, \quad \|J_E\|_{0,\infty,\hat{E}} \sim h^d, \quad \text{and} \quad \|J_{F_E^{-1}}\|_{0,\infty,\hat{E}} \sim h^{-d} \quad \forall\, E \in \mathcal{T}_h, \tag{2.14}$$

where the notation $a \sim b$ means that there exist positive constants c_0 and c_1 independent of h such that $c_0 b \le a \le c_1 b$.

2.3. Mixed finite element spaces. Let $\mathbf{V}_h \times W_h$ be the lowest order BDM_1 MFE spaces [14, 15]. On the reference unit square these spaces are defined as

$$\begin{aligned} \hat{\mathbf{V}}(\hat{E}) &= P_1(\hat{E})^2 + r\ \mathrm{curl}(\hat{x}^2\hat{y}) + s\ \mathrm{curl}(\hat{x}\hat{y}^2) \\ &= \begin{pmatrix} \alpha_1\hat{x} + \beta_1\hat{y} + \gamma_1 + r\hat{x}^2 + 2s\hat{x}\hat{y} \\ \alpha_2\hat{x} + \beta_2\hat{y} + \gamma_2 - 2r\hat{x}\hat{y} - s\hat{y}^2 \end{pmatrix}, \quad \hat{W}(\hat{E}) = P_0(\hat{E}), \end{aligned} \tag{2.15}$$

where $\alpha_1, \alpha_2, \beta_1, \beta_2, \gamma_1, \gamma_2, s, r$ are real constants and P_k denotes the space of polynomials of degree $\le k$. In the case where the reference element $\hat{E}$ is the unit triangle or tetrahedron, the BDM_1 spaces are defined as

$$\hat{\mathbf{V}}(\hat{E}) = P_1(\hat{E})^d, \quad \hat{W}(\hat{E}) = P_0(\hat{E}). \tag{2.16}$$

Note that in all three cases $\hat{\nabla} \cdot \hat{\mathbf{V}}(\hat{E}) = \hat{W}(\hat{E})$ and that for all $\hat{\mathbf{v}} \in \hat{\mathbf{V}}(\hat{E})$ and for any edge (or face) $\hat{e}$ of $\hat{E}$,

$$\hat{\mathbf{v}} \cdot \hat{\mathbf{n}}_{\hat{e}} \in P_1(\hat{e}).$$

It is well known [14, 15] that the degrees of freedom for $\hat{\mathbf{V}}(\hat{E})$ can be chosen to be the values of $\hat{\mathbf{v}} \cdot \hat{\mathbf{n}}_{\hat{e}}$ at any two points on each edge $\hat{e}$ if $\hat{E}$ is the unit triangle or the unit square, or any three points on each face $\hat{e}$ if $\hat{E}$ is the unit tetrahedron. *We choose these points to be the vertices of* $\hat{e}$; see Figure 2.2 for the quadrilateral case. This choice is motivated by the requirement of accuracy and certain orthogonalities for the quadrature rule introduced in the next section.

The BDM_1 spaces on any element $E \in \mathcal{T}_h$ are defined via the transformations

$$\mathbf{v} \leftrightarrow \hat{\mathbf{v}} : \mathbf{v} = \frac{1}{J_E} DF_E \hat{\mathbf{v}} \circ F_E^{-1}, \quad w \leftrightarrow \hat{w} : w = \hat{w} \circ F_E^{-1}.$$

The vector transformation is known as the Piola transformation. It is designed to preserve the normal components of the velocity vectors on the edges (faces) and satisfies the important properties [15]

$$(\nabla \cdot \mathbf{v}, w)_E = (\hat{\nabla} \cdot \hat{\mathbf{v}}, \hat{w})_{\hat{E}} \qquad \text{and} \qquad \langle \mathbf{v} \cdot \mathbf{n}_e, w \rangle_e = \langle \hat{\mathbf{v}} \cdot \hat{\mathbf{n}}_{\hat{e}}, \hat{w} \rangle_{\hat{e}}. \tag{2.17}$$

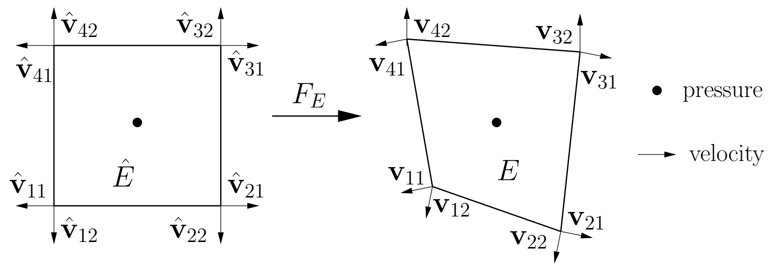

FIG. 2.2. *Degrees of freedom and basis functions for the BDM_1 spaces on quadrilaterals.*

Moreover, (2.13) implies

$$\mathbf{v}\cdot\mathbf{n}_e = \frac{1}{J_E}DF_E\hat{\mathbf{v}}\cdot\frac{1}{|e|}J_E(DF_E^{-1})^T\hat{\mathbf{n}}_{\hat{e}} = \frac{1}{|e|}\hat{\mathbf{v}}\cdot\hat{\mathbf{n}}_{\hat{e}}. \tag{2.18}$$

Also note that the first equation in (2.17) and $(\nabla\cdot\mathbf{v},w)_E = (\widehat{\nabla\cdot\mathbf{v}},\hat{w}J_E)_{\hat{E}}$ imply

$$\nabla\cdot\mathbf{v} = \left(\frac{1}{J_E}\hat{\nabla}\cdot\hat{\mathbf{v}}\right)\circ F_E^{-1}(\mathbf{x}). \tag{2.19}$$

Therefore on quadrilaterals $\nabla\cdot\mathbf{v}|_E \neq$ constant.

The BDM_1 spaces on $\mathcal{T}_h$ are given by

$$\begin{aligned}\mathbf{V}_h &= \{\mathbf{v}\in\mathbf{V}\colon \quad \mathbf{v}|_E \leftrightarrow \hat{\mathbf{v}},\ \hat{\mathbf{v}}\in\hat{\mathbf{V}}(\hat{E}) \quad \forall E\in\mathcal{T}_h\},\\ W_h &= \{w\in W\colon \quad w|_E\leftrightarrow\hat{w},\ \hat{w}\in\hat{W}(\hat{E}) \quad \forall E\in\mathcal{T}_h\}.\end{aligned} \tag{2.20}$$

It is known [14, 15, 32] that there exists a projection operator Π from $\mathbf{V}\cap(H^1(\Omega))^d$ onto $\mathbf{V}_h$ satisfying

$$(\nabla\cdot(\Pi\mathbf{q}-\mathbf{q}),w) = 0 \qquad \forall\, w\in W_h. \tag{2.21}$$

The operator Π is defined locally on each element E by

$$\Pi\mathbf{q}\leftrightarrow\widehat{\Pi\mathbf{q}}, \quad \widehat{\Pi\mathbf{q}} = \hat{\Pi}\hat{\mathbf{q}}, \tag{2.22}$$

where $\hat{\Pi} : (H^1(\hat{E}))^d \to \hat{\mathbf{V}}(\hat{E})$ is the reference element projection operator satisfying

$$\forall\,\hat{e}\subset\partial\hat{E}, \qquad \langle(\hat{\Pi}\hat{\mathbf{q}}-\hat{\mathbf{q}})\cdot\hat{\mathbf{n}},\hat{p}_1\rangle_{\hat{e}} = 0 \qquad \forall\,\hat{p}_1\in P_1(\hat{e}). \tag{2.23}$$

To see that $\Pi\mathbf{q}\cdot\mathbf{n} = 0$ on Γ_N if $\mathbf{q}\cdot\mathbf{n} = 0$ on Γ_N, note that for any $e\in\Gamma_N$ and for all $p_1\leftrightarrow\hat{p}_1\in P_1(\hat{e})$,

$$\langle\Pi\mathbf{q}\cdot\mathbf{n},p_1\rangle_e = \langle\widehat{\Pi\mathbf{q}}\cdot\hat{\mathbf{n}},\hat{p}_1\rangle_{\hat{e}} = \langle\hat{\Pi}\hat{\mathbf{q}}\cdot\hat{\mathbf{n}},\hat{p}_1\rangle_{\hat{e}} = \langle\hat{\mathbf{q}}\cdot\hat{\mathbf{n}},\hat{p}_1\rangle_{\hat{e}} = 0,$$

implying $\Pi\mathbf{q}\cdot\mathbf{n} = 0$, where we have used (2.17), (2.22), and (2.23).

In addition to the mixed projection operator Π onto $\mathbf{V}_h$, we will use a similar projection operator onto the lowest order Raviart–Thomas spaces [27, 15]. The RT_0 spaces are defined on the unit square as

$$\hat{\mathbf{V}}^0(\hat{E}) = \begin{pmatrix}\alpha_1+\beta_1\hat{x}\\ \alpha_2+\beta_2\hat{y}\end{pmatrix}, \quad \hat{W}^0(\hat{E}) = P_0(\hat{E}), \tag{2.24}$$

and on the unit triangle as

$$\hat{\mathbf{V}}^0(\hat{E}) = \begin{pmatrix} \alpha_1 + \beta\hat{x} \\ \alpha_2 + \beta\hat{y} \end{pmatrix}, \quad \hat{W}^0(\hat{E}) = P_0(\hat{E}). \tag{2.25}$$

On the unit tetrahedron $\hat{\mathbf{V}}^0(\hat{E})$ has an additional component $\alpha_3 + \beta\hat{z}$. In all cases $\hat{\nabla} \cdot \hat{\mathbf{V}}^0(\hat{E}) = \hat{W}^0(\hat{E})$ and $\hat{\mathbf{v}} \cdot \hat{\mathbf{n}}_{\hat{e}} \in P_0(\hat{e})$. The degrees of freedom of $\hat{\mathbf{V}}^0(\hat{E})$ are the values of $\hat{\mathbf{v}} \cdot \hat{\mathbf{n}}_{\hat{e}}$ at the midpoints of all edges (faces) $\hat{e}$. The projection operator $\hat{\Pi}_0 : (H^1(\hat{E}))^d \to \hat{\mathbf{V}}^0(\hat{E})$ satisfies

$$\forall\, \hat{e} \subset \partial\hat{E}, \qquad \langle(\hat{\Pi}_0\hat{\mathbf{q}} - \hat{\mathbf{q}}) \cdot \hat{\mathbf{n}}, \hat{p}_0\rangle_{\hat{e}} = 0 \qquad \forall\, \hat{p}_0 \in P_0(\hat{e}). \tag{2.26}$$

The spaces $\mathbf{V}_h^0$ and W_h^0 on $\mathcal{T}_h$ and the projection operator $\Pi_0 : (H^1(\Omega))^d \to \mathbf{V}_h^0$ are defined similarly to the case of BDM$_1$ spaces. Note that $\mathbf{V}_h^0 \subset \mathbf{V}_h$ and $W_h^0 = W_h$. It follows immediately from the definition of Π_0 that

$$\nabla \cdot \mathbf{v} = \nabla \cdot \Pi_0\mathbf{v} \quad \forall\, \mathbf{v} \in \mathbf{V}_h \tag{2.27}$$

and

$$\|\Pi_0\mathbf{v}\| \le C\|\mathbf{v}\| \quad \forall\, \mathbf{v} \in \mathbf{V}_h. \tag{2.28}$$

2.4. The BDM$_1$ method. The BDM$_1$ mixed finite element method is based on approximating the variational formulation (2.6)–(2.7) in the discrete spaces $\mathbf{V}_h \times W_h$: find $\mathbf{u}_h^{bdm} \in \mathbf{V}_h$ and $p_h^{bdm} \in W_h$ such that

$$(K^{-1}\mathbf{u}_h^{bdm}, \mathbf{v}) = (p_h^{bdm}, \nabla \cdot \mathbf{v}) - \langle g, \mathbf{v} \cdot \mathbf{n}\rangle_{\Gamma_D}, \quad \mathbf{v} \in \mathbf{V}_h, \tag{2.29}$$

$$(\nabla \cdot \mathbf{u}_h^{bdm}, w) = (f, w), \quad w \in W_h. \tag{2.30}$$

The method has a unique solution and is second order accurate for the velocity and first order accurate for the pressure in L^2-norms on affine grids [14, 32]. It handles well discontinuous coefficients due to the presence of K^{-1} in the mass matrix. A drawback is that the resulting algebraic system is a large coupled velocity-pressure system of a saddle point problem type. In the next section we develop a quadrature rule that allows for local elimination of the velocities and results in a positive definite cell-centered pressure matrix.

2.5. A quadrature rule. For $\mathbf{q}$, $\mathbf{v} \in \mathbf{V}_h$, define the global quadrature rule

$$(K^{-1}\mathbf{q}, \mathbf{v})_Q \equiv \sum_{E \in \mathcal{T}_h} (K^{-1}\mathbf{q}, \mathbf{v})_{Q,E}.$$

The integration on any element E is performed by mapping to the reference element $\hat{E}$. The quadrature rule is defined on $\hat{E}$. Using the definition (2.20) of the finite element spaces and omitting the subscript E, we have

$$\begin{aligned} \int_E K^{-1}\mathbf{q} \cdot \mathbf{v}\, d\mathbf{x} &= \int_{\hat{E}} \hat{K}^{-1} \frac{1}{J} DF\hat{\mathbf{q}} \cdot \frac{1}{J} DF\hat{\mathbf{v}}\, J\, d\hat{\mathbf{x}} \\ &= \int_{\hat{E}} \frac{1}{J} DF^T \hat{K}^{-1} DF\hat{\mathbf{q}} \cdot \hat{\mathbf{v}}\, d\hat{\mathbf{x}} \equiv \int_{\hat{E}} \mathcal{K}^{-1}\hat{\mathbf{q}} \cdot \hat{\mathbf{v}}\, d\hat{\mathbf{x}}, \end{aligned}$$

where

$$\mathcal{K} = J DF^{-1} \hat{K} (DF^{-1})^T. \tag{2.31}$$

Clearly, due to (2.14),

$$\|\mathcal{K}\|_{0,\infty,\hat{E}} \sim h^{d-2}\|K\|_{0,\infty,E} \quad \text{and} \quad \|\mathcal{K}^{-1}\|_{0,\infty,\hat{E}} \sim h^{2-d}\|K^{-1}\|_{0,\infty,E}. \tag{2.32}$$

The quadrature rule on an element E is defined as

$$(K^{-1}\mathbf{q},\mathbf{v})_{Q,E} \equiv (\mathcal{K}^{-1}\hat{\mathbf{q}},\hat{\mathbf{v}})_{\hat{Q},\hat{E}} \equiv \frac{|\hat{E}|}{s}\sum_{i=1}^{s}\mathcal{K}^{-1}(\hat{\mathbf{r}}_i)\hat{\mathbf{q}}(\hat{\mathbf{r}}_i)\cdot\hat{\mathbf{v}}(\hat{\mathbf{r}}_i), \tag{2.33}$$

where $s=3$ for the unit triangle and $s=4$ for the unit square or the unit tetrahedron. Note that on the unit square this is the trapezoidal quadrature rule.

The corner vector $\hat{\mathbf{q}}(\hat{\mathbf{r}}_i)$ is uniquely determined by its normal components to the two edges (or three faces) that share that vertex. Recall that we chose the velocity degrees of freedom on any edge (face) $\hat{e}$ to be the normal components at the vertices of $\hat{e}$. Therefore, there are two (three) degrees of freedom associated with each corner $\hat{\mathbf{r}}_i$ and they uniquely determine the corner vector $\hat{\mathbf{q}}(\hat{\mathbf{r}}_i)$. More precisely,

$$\hat{\mathbf{q}}(\hat{\mathbf{r}}_i) = \sum_{j=1}^{d}\hat{\mathbf{q}}\cdot\hat{\mathbf{n}}_{ij}(\hat{\mathbf{r}}_i)\hat{\mathbf{n}}_{ij},$$

where $\hat{\mathbf{n}}_{ij}$, $j=1,\dots,d$, are the outward unit normal vectors to the two edges (three faces) intersecting at $\hat{\mathbf{r}}_i$, and $\hat{\mathbf{q}}\cdot\hat{\mathbf{n}}_{ij}(\hat{\mathbf{r}}_i)$ are the velocity degrees of freedom associated with this corner. Let us denote the basis functions associated with $\hat{\mathbf{r}}_i$ by $\hat{\mathbf{v}}_{ij}$, $j = 1,\dots,d$; see Figure 2.2, i.e.,

$$\hat{\mathbf{v}}_{ij}\cdot\hat{\mathbf{n}}_{ij}(\hat{\mathbf{r}}_i)=1,\ \ \hat{\mathbf{v}}_{ij}\cdot\hat{\mathbf{n}}_{ik}(\hat{\mathbf{r}}_i)=0,\ k\neq j,\ \text{and}\ \hat{\mathbf{v}}_{ij}\cdot\hat{\mathbf{n}}_{lk}(\hat{\mathbf{r}}_l)=0,\ l\neq i,\ k=1,\dots,d.$$

Clearly the quadrature rule (2.33) couples only the two (or three) basis functions associated with a corner. On the unit square, for example,

$$(\mathcal{K}^{-1}\hat{\mathbf{v}}_{11},\hat{\mathbf{v}}_{11})_{\hat{Q},\hat{E}} = \frac{\mathcal{K}^{-1}_{11}(\hat{\mathbf{r}}_1)}{4}, \quad (\mathcal{K}^{-1}\hat{\mathbf{v}}_{11},\hat{\mathbf{v}}_{12})_{\hat{Q},\hat{E}} = \frac{\mathcal{K}^{-1}_{12}(\hat{\mathbf{r}}_1)}{4}, \tag{2.34}$$

and

$$(\mathcal{K}^{-1}\hat{\mathbf{v}}_{11},\hat{\mathbf{v}}_{ij})_{\hat{Q},\hat{E}} = 0 \quad \forall\, ij\neq 11,12. \tag{2.35}$$

Remark 2.1. The quadrature rule can be defined directly on an element E. It is easy to see from (2.10) and (2.12) that on simplicial elements

$$(K^{-1}\mathbf{q},\mathbf{v})_{Q,E} = \frac{|E|}{s}\sum_{i=1}^{s}K^{-1}(\mathbf{r}_i)\mathbf{q}(\mathbf{r}_i)\cdot\mathbf{v}(\mathbf{r}_i), \tag{2.36}$$

and on quadrilaterals

$$(K^{-1}\mathbf{q},\mathbf{v})_{Q,E} = \frac{1}{2}\sum_{i=1}^{4}|T_i|K^{-1}(\mathbf{r}_i)\mathbf{q}(\mathbf{r}_i)\cdot\mathbf{v}(\mathbf{r}_i). \tag{2.37}$$

The above quadrature rules are closely related to some inner products used in the mimetic finite difference methods [23]. We note that in the case of quadrilaterals, it is simpler to evaluate the quadrature rule on the reference element $\hat{E}$.

Denote the element quadrature error by

$$\sigma_E(K^{-1}\mathbf{q},\mathbf{v}) \equiv (K^{-1}\mathbf{q},\mathbf{v})_E - (K^{-1}\mathbf{q},\mathbf{v})_{Q,E} \tag{2.38}$$

and define the global quadrature error by $\sigma(K^{-1}\mathbf{q},\mathbf{v})|_E = \sigma_E(K^{-1}\mathbf{q},\mathbf{v})$. Similarly, denote the quadrature error on the reference element by

$$\hat{\sigma}_{\hat{E}}(\mathcal{K}^{-1}\hat{\mathbf{q}},\hat{\mathbf{v}}) \equiv (\mathcal{K}^{-1}\hat{\mathbf{q}},\hat{\mathbf{v}})_{\hat{E}} - (\mathcal{K}^{-1}\hat{\mathbf{q}},\hat{\mathbf{v}})_{\hat{Q},\hat{E}}. \tag{2.39}$$

The next two lemmas will be used in the analysis.

LEMMA 2.1. *On simplicial elements, if* $\mathbf{q} \in \mathbf{V}_h(E)$, *then*

$$\sigma_E(\mathbf{q},\mathbf{v}_0) = 0 \quad \textit{for all constant vectors } \mathbf{v}_0.$$

Proof. It is enough to consider $\mathbf{v}_0 = (1,0)^T$ or $\mathbf{v}_0 = (1,0,0)^T$; the arguments for the other cases are similar. We have

$$(\mathbf{q},\mathbf{v}_0)_{Q,E} = \frac{|E|}{s}\sum_{i=1}^{s} q_1(\mathbf{r}_i) = \int_E \mathbf{q}\cdot\mathbf{v}_0\,\mathrm{d}\mathbf{x},$$

using that the quadrature rule $(\varphi)_E = \frac{|E|}{s}\sum_{i=1}^{s}\varphi(\mathbf{r}_i)$ is exact for linear functions. □

LEMMA 2.2. *On the reference square, for any* $\hat{\mathbf{q}} \in \hat{\mathbf{V}}(\hat{E})$,

$$(\hat{\mathbf{q}} - \hat{\Pi}_0\hat{\mathbf{q}},\hat{\mathbf{v}}_0)_{\hat{Q},\hat{E}} = 0 \quad \textit{for all constant vectors } \hat{\mathbf{v}}_0. \tag{2.40}$$

Proof. On any edge $\hat{e}$, if the degrees of freedom of $\hat{\mathbf{q}}$ are $\hat{q}_{\hat{e},1}$ and $\hat{q}_{\hat{e},2}$, then (2.26) and an application of the trapezoidal quadrature rule imply that $\hat{\Pi}_0\hat{\mathbf{q}}|_{\hat{e}} = (\hat{q}_{\hat{e},1} + \hat{q}_{\hat{e},2})/2$. The assertion of the lemma follows from a simple calculation, using (2.33). □

2.6. The multipoint flux mixed finite element method. We are now ready to define our method. We seek $\mathbf{u}_h \in \mathbf{V}_h$ and $p_h \in W_h$ such that

$$(K^{-1}\mathbf{u}_h,\mathbf{v})_Q = (p_h,\nabla\cdot\mathbf{v}) - \langle g,\mathbf{v}\cdot\mathbf{n}\rangle_{\Gamma_D}, \quad \mathbf{v}\in\mathbf{V}_h, \tag{2.41}$$

$$(\nabla\cdot\mathbf{u}_h, w) = (f,w), \quad w \in W_h. \tag{2.42}$$

Remark 2.2. We call the method (2.41)–(2.42) a MFMFE method, since it is related to the MPFA method.

To prove that (2.41)–(2.42) is well posed, we first show that the quadrature rule (2.33) produces a coercive bilinear form. We will need the following auxiliary result.

LEMMA 2.3. *If* $E \in \mathcal{T}_h$ *and* $\mathbf{q} \in (L^2(E))^d$, *then*

$$\|\mathbf{q}\|_E \sim h^{\frac{2-d}{2}}\|\hat{\mathbf{q}}\|_{\hat{E}}. \tag{2.43}$$

Proof. The assertion of the lemma follows from the relations

$$\int_E \mathbf{q}\cdot\mathbf{q}\,\mathrm{d}\mathbf{x} = \int_{\hat{E}} \frac{1}{J}DF\hat{\mathbf{q}}\cdot\frac{1}{J}DF\hat{\mathbf{q}}\,J\,\mathrm{d}\hat{\mathbf{x}},$$

$$\int_{\hat{E}} \hat{\mathbf{q}}\cdot\hat{\mathbf{q}}\,\mathrm{d}\hat{\mathbf{x}} = \int_E \frac{1}{J_{F^{-1}}}DF^{-1}\mathbf{q}\cdot\frac{1}{J_{F^{-1}}}DF^{-1}\mathbf{q}J_{F^{-1}}\,\mathrm{d}\mathbf{x},$$

and bounds (2.14). □

LEMMA 2.4. *There exists a positive constant C independent of h such that*

$$(K^{-1}\mathbf{q},\mathbf{q})_Q \geq C\|\mathbf{q}\|^2 \quad \forall \mathbf{q}\in \mathbf{V}_h. \tag{2.44}$$

Proof. Let $\mathbf{q} = \sum_{i=1}^s \sum_{j=1}^d q_{ij}\mathbf{v}_{ij}$ on an element E. Using (2.36)–(2.37) and (2.5) we obtain

$$(K^{-1}\mathbf{q},\mathbf{q})_{Q,E} \geq C\frac{|E|}{k_1}\sum_{i=1}^s \mathbf{q}(\mathbf{r}_i)\cdot\mathbf{q}(\mathbf{r}_i) \geq C\frac{|E|}{k_1}\sum_{i=1}^s\sum_{j=1}^d q_{ij}^2.$$

On the other hand,

$$\|\mathbf{q}\|_E^2 = \left(\sum_{i=1}^s\sum_{j=1}^d q_{ij}\mathbf{v}_{ij}, \sum_{k=1}^s\sum_{l=1}^d q_{kl}\mathbf{v}_{kl}\right) \leq C|E|\sum_{i=1}^s\sum_{j=1}^d q_{ij}^2.$$

A combination of the above two estimates implies the assertion of the lemma. ∎

COROLLARY 2.5. *The bilinear form $(K^{-1}\mathbf{q},\mathbf{v})_Q$ is an inner product in $\mathbf{V}_h$ and $(K^{-1}\mathbf{q},\mathbf{q})_Q^{1/2}$ is a norm in $\mathbf{V}_h$ equivalent to $\|\cdot\|$.*

Proof. Since $(K^{-1}\mathbf{q},\mathbf{v})_Q$ is linear and symmetric, Lemma 2.4 implies that it is an inner product and that $(K^{-1}\mathbf{q},\mathbf{q})_Q^{1/2}$ is a norm in $\mathbf{V}_h$. Let us denote this norm by $\|\cdot\|_{Q,K^{-1}}$. It remains to show that it is bounded above by $\|\cdot\|$. Using (2.32), (2.5), the equivalence of norms on reference element $\hat{E}$, and (2.43), we have that for all $\mathbf{q}\in\mathbf{V}_h$

$$(K^{-1}\mathbf{q},\mathbf{q})_{Q,E} = (\mathcal{K}^{-1}\hat{\mathbf{q}},\hat{\mathbf{q}})_{\hat{Q},\hat{E}} \leq C\frac{h^{2-d}}{k_0}\|\hat{\mathbf{q}}\|_{\hat{E}}^2 \leq C\|\mathbf{q}\|_E^2,$$

which, combined with (2.44), implies that

$$c_0\|\mathbf{q}\| \leq \|\mathbf{q}\|_{Q,K^{-1}} \leq c_1\|\mathbf{q}\| \tag{2.45}$$

for some positive constants c_0 and c_1. ∎

Remark 2.3. The results of Lemma 2.4 and Corollary 2.5 hold if K^{-1} is replaced by any symmetric and positive definite matrix M.

We are now ready to establish the solvability of (2.41)–(2.42).

LEMMA 2.6. *The MFMFE method* (2.41)–(2.42) *has a unique solution.*

Proof. Since (2.41)–(2.42) is a square system, it is enough to show uniqueness. Let $f=0$, $g=0$, and take $\mathbf{v}=\mathbf{u}_h$ and $w=p_h$. This implies that $(K^{-1}\mathbf{u}_h,\mathbf{u}_h)_Q=0$, and therefore $\mathbf{u}_h=0$, due to (2.44). We now consider the auxiliary problem

$$\begin{aligned} -\nabla\cdot K\nabla\phi &= -p_h \quad \text{in} \quad \Omega,\\ \phi &= 0 \quad \text{on} \quad \Gamma_D,\\ -K\nabla\phi\cdot\mathbf{n} &= 0 \quad \text{on} \quad \Gamma_N. \end{aligned}$$

The choice $\mathbf{v}=\Pi K\nabla\phi\in\mathbf{V}_h$ in (2.41) gives

$$0 = (p_h,\nabla\cdot\Pi K\nabla\phi) = (p_h,\nabla\cdot K\nabla\phi) = \|p_h\|^2,$$

therefore $p_h=0$. ∎

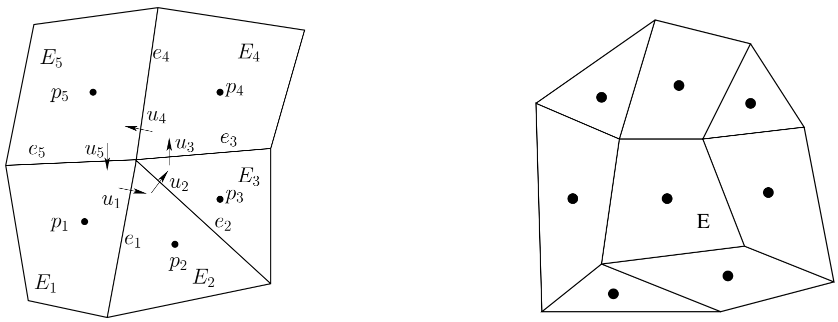

A. Five elements sharing a vertex.

B. Pressure stencil.

FIG. 2.3. *Interactions of the degrees of freedom in MFMFE.*

2.7. Reduction to a cell-centered stencil. We next describe how the MFMFE method reduces to a system for the pressures at the cell centers. Let us consider any interior vertex $\mathbf{r}$ and suppose that it is shared by k elements $E_1, \dots, E_k$; see Figure 2.3(A) for a specific example with 5 elements. We denote the edges (faces) that share the vertex by $e_1, \dots, e_k$, the velocity basis functions on these edges (faces) that are associated with the vertex by $\mathbf{v}_1, \dots, \mathbf{v}_k$, and the corresponding values of the normal components of $\mathbf{u}_h$ by $u_1, \dots, u_k$. Note that for clarity the normal velocities on Figure 2.3(A) are drawn at a distance from the vertex.

Since the quadrature rule $(K^{-1}\cdot, \cdot)_Q$ localizes the basis functions interaction (see (2.34)–(2.35)), taking $\mathbf{v} = \mathbf{v}_1$ in (2.41), for example, will only lead to coupling u_1 with u_5 and u_2. Similarly, u_2 will only be coupled with u_1 and u_3, etc. Therefore, the k equations obtained from taking $\mathbf{v} = \mathbf{v}_1, \dots, \mathbf{v}_k$ form a linear system for $u_1, \dots, u_k$.

PROPOSITION 2.7. *The $k \times k$ local linear system described above is symmetric and positive definite.*

Proof. The system is obtained by taking $\mathbf{v} = \mathbf{v}_1, \dots, \mathbf{v}_k$ in (2.41). On the left-hand side we have

$$(K^{-1}\mathbf{u}_h, \mathbf{v}_i)_Q = \sum_{j=1}^{k} u_j (K^{-1}\mathbf{v}_j, \mathbf{v}_i)_Q \equiv \sum_{j=1}^{k} a_{ij} u_j, \quad i = 1, \dots, k.$$

Using Corollary 2.5 we conclude that the matrix $\bar{A} = \{a_{ij}\}$ is symmetric and positive definite. ◻

Solving the small $k \times k$ linear system allows us to express the velocities u_i in terms of the cell-centered pressures p_i, $i = 1, \dots, k$. Substituting these expressions into the mass conservation equation (2.42) leads to a cell-centered stencil. The pressure in each element E is coupled with the pressures in the elements that share a vertex with E; see Figure 2.3(B).

For any vertex on the boundary $\partial\Omega$, the size of the local linear system equals the number of non-Neumann (interior or Dirichlet) edges/faces that share that vertex. Inverting the local system allows one to express the velocities in terms of the element pressures and the boundary data.

We use the example in Figure 2.3(A) to describe the CCFD equations obtained from the above procedure. Taking $\mathbf{v} = \mathbf{v}_1$ in (2.41), on the left-hand side we have

$$(K^{-1}\mathbf{u}_h, \mathbf{v}_1)_Q = (K^{-1}\mathbf{u}_h, \mathbf{v}_1)_{Q,E_1} + (K^{-1}\mathbf{u}_h, \mathbf{v}_1)_{Q,E_2}. \quad (2.46)$$

The first term on the right in (2.46) gives

$$\begin{aligned}(K^{-1}\mathbf{u}_h,\mathbf{v}_1)_{Q,E_1} &= (\mathcal{K}^{-1}\hat{\mathbf{u}}_h,\hat{\mathbf{v}}_1)_{\hat{Q},\hat{E}}\\ &= \frac{1}{4}(\mathcal{K}^{-1}_{11,E_1}\hat{u}_1\hat{v}_{1,1}+\mathcal{K}^{-1}_{12,E_1}\hat{u}_5\hat{v}_{1,1})\\ &= \frac{1}{4}(\mathcal{K}^{-1}_{11,E_1}|e_1|u_1+\mathcal{K}^{-1}_{12,E_1}|e_5|u_5)|e_1|,\end{aligned}\tag{2.47}$$

where we have used (2.18) for the last equality. Here $\mathcal{K}^{-1}_{ij,E_1}$ denotes a component of $\mathcal{K}^{-1}$ in E_1 and all functions are evaluated at the vertex of $\hat{E}$ corresponding to vertex $\mathbf{r}$ in the mapping F_{E_1}. Similarly,

$$(K^{-1}\mathbf{u}_h,\mathbf{v}_1)_{Q,E_2} = \frac{1}{6}(\mathcal{K}^{-1}_{11,E_2}|e_1|u_1+\mathcal{K}^{-1}_{12,E_2}|e_2|u_2)|e_1|.\tag{2.48}$$

For the right-hand side of (2.41) we write

$$\begin{aligned}(p_h,\nabla\cdot\mathbf{v}_1) &= (p_h,\nabla\cdot\mathbf{v}_1)_{E_1}+(p_h,\nabla\cdot\mathbf{v}_1)_{E_2}\\ &= \langle p_h,\mathbf{v}_1\cdot\mathbf{n}_{E_1}\rangle_{e_1}+\langle p_h,\mathbf{v}_1\cdot\mathbf{n}_{E_2}\rangle_{e_1}\\ &= \langle \hat{p}_h,\hat{\mathbf{v}}_1\cdot\hat{\mathbf{n}}_{E_1}\rangle_{\hat{e}_1}+\langle \hat{p}_h,\hat{\mathbf{v}}_1\cdot\hat{\mathbf{n}}_{E_2}\rangle_{\hat{e}_1}\\ &= \frac{1}{2}(p_1-p_2)|e_1|,\end{aligned}\tag{2.49}$$

where we have used the trapezoidal rule for the integrals on $\hat{e}_1$, which is exact since $\hat{p}_h$ is constant and $\hat{\mathbf{v}}_1\cdot\hat{\mathbf{n}}$ is linear. A combination of (2.46)–(2.49) gives the equation

$$\left(\frac{1}{2}\mathcal{K}^{-1}_{11,E_1}+\frac{1}{3}\mathcal{K}^{-1}_{11,E_2}\right)|e_1|u_1+\frac{1}{2}\mathcal{K}^{-1}_{12,E_1}|e_5|u_5+\frac{1}{3}\mathcal{K}^{-1}_{12,E_2}|e_2|u_2 = p_1-p_2.$$

The other four equations of the local system for $u_1,\dots,u_5$ are obtained similarly.

We end the section with a statement about an important property of the CCFD algebraic system.

PROPOSITION 2.8. *The CCFD system for the pressure obtained from* (2.41)–(2.42) *using the procedure described above is symmetric and positive definite.*

Proof. Let $\{\mathbf{v}_i\}$ and $\{w_j\}$ be the bases of $\mathbf{V}_h$ and W_h, respectively. The algebraic system that arises from (2.41)–(2.42) is of the form

$$\begin{pmatrix} A & B^T\\ B & 0\end{pmatrix}\begin{pmatrix} U\\ P\end{pmatrix} = \begin{pmatrix} G\\ F\end{pmatrix},\tag{2.50}$$

where $A_{ij} = (K^{-1}\mathbf{v}_i,\mathbf{v}_j)_Q$ and $B_{ij} = -(\nabla\cdot\mathbf{v}_i,w_j)$. The matrix A is block-diagonal with symmetric and positive definite blocks, as noted in Proposition 2.7. The elimination of U leads to a system for P with a matrix

$$BA^{-1}B^T,$$

which is symmetric and positive semidefinite. In the proof of Lemma 2.6 we showed that $B^TP = 0$ implies $P = 0$. Therefore $BA^{-1}B^T$ is positive definite. ∎

3. Velocity error analysis. Although our method can be defined and is well posed on general quadrilaterals (see section 2), for the convergence analysis we need to impose a restriction on the element geometry. This is due to the reduced approximation properties of the MFE spaces on general quadrilaterals [8]. The restriction is not needed for theoretical purpose only; deterioration of convergence is observed computationally as well [3].

For the remainder of the paper we will assume that the quadrilateral elements are $O(h^2)$-perturbations of parallelograms:

$$\|\mathbf{r}_{34} - \mathbf{r}_{21}\| \le Ch^2. \tag{3.1}$$

We call such elements h^2-parallelograms, following the terminology from [21]. Elements of this type are obtained by uniform refinements of a general quadrilateral grid. It is not difficult to check that in this case $||T_2| - |T_1|| \le Ch^3$, $||T_4| - |T_1|| \le Ch^3$, and

$$|DF_E|_{1,\infty,\hat{E}} \le Ch^2 \quad \text{and} \quad \left|\frac{1}{J_E} DF_E\right|_{j,\infty,\hat{E}} \le Ch^{j-1}, \quad j = 1, 2. \tag{3.2}$$

In this section we establish first-order convergence for the velocity. We start with several auxiliary results that will be used in the analysis.

In addition to the mixed projection operators defined earlier, we will also make use of the L^2-orthogonal projection onto W_h: for any $\phi \in L^2(\Omega)$, let $\mathcal{Q}_h \phi \in W_h$ satisfy

$$(\phi - \mathcal{Q}_h \phi, w) = 0 \qquad \forall w \in W_h.$$

We state several well-known approximation properties of the projection operators. On simplices and h^2-parallelograms,

$$\|\phi - \mathcal{Q}_h \phi\| \le C\|\phi\|_r h^r, \quad 0 \le r \le 1, \tag{3.3}$$

$$\|\mathbf{q} - \Pi \mathbf{q}\| \le C\|\mathbf{q}\|_r h^r, \quad 1 \le r \le 2, \tag{3.4}$$

$$\|\mathbf{q} - \Pi_0 \mathbf{q}\| \le C\|\mathbf{q}\|_1 h, \tag{3.5}$$

$$\|\nabla \cdot (\mathbf{q} - \Pi \mathbf{q})\| + \|\nabla \cdot (\mathbf{q} - \Pi_0 \mathbf{q})\| \le C\|\nabla \cdot \mathbf{q}\|_r h^r, \quad 0 \le r \le 1. \tag{3.6}$$

Bound (3.3) is a standard L^2-projection approximation results [18]; bounds (3.4), (3.5), and (3.6) can be found in [15, 28] for affine elements and [32, 8] for h^2-parallelograms. We note that on general quadrilaterals bounds (3.3) and (3.5) are also true, while bounds (3.4) and (3.6) are only valid for $r = 1$ and $r = 0$, respectively [8].

It was shown in [21, Lemma 5.5] that on h^2-parallelograms, for $\mathbf{u} \in H^j(E)$,

$$|\hat{\mathbf{u}}|_{j,\hat{E}} \le Ch^j \|\mathbf{u}\|_{j,E}, \quad j \ge 0. \tag{3.7}$$

We will make use of the following continuity bounds for Π and Π_0.

LEMMA 3.1. *For all elements E there exists a constant C independent of h such that*

$$\|\Pi \mathbf{q}\|_{j,E} \le C\|\mathbf{q}\|_{j,E} \quad \forall \mathbf{q} \in (H^j(E))^d, \quad j = 1, 2, \tag{3.8}$$

$$\|\Pi_0 \mathbf{q}\|_{1,E} \le C\|\mathbf{q}\|_{1,E} \quad \forall \mathbf{q} \in (H^1(E))^d. \tag{3.9}$$

Proof. The proof uses the inverse inequality

$$\|\mathbf{v}\|_{j,E} \le Ch^{-1}\|\mathbf{v}\|_{j-1,E}, \quad j = 1, 2 \quad \forall E \in \mathcal{T}_h, \mathbf{v} \in \mathbf{V}_h(E), \tag{3.10}$$

which is well known for affine elements [18] and can be shown for quadrilaterals via mapping to the reference element $\hat{E}$ and using the standard inverse inequality on $\hat{E}$; see [11] for details.

Let $\bar{\mathbf{q}}$ be the $L^2(E)$-projection of $\mathbf{q}$ onto the space of constant vectors on E. Using (3.10), we have

$$|\Pi\mathbf{q}|_{1,E} = |\Pi\mathbf{q} - \bar{\mathbf{q}}|_{1,E} \le Ch^{-1}\|\Pi\mathbf{q} - \bar{\mathbf{q}}\|_E \\ \le Ch^{-1}(\|\Pi\mathbf{q} - \mathbf{q}\|_E + \|\mathbf{q} - \bar{\mathbf{q}}\|_E) \le C\|\mathbf{q}\|_{1,E},$$

where we have used the approximation properties (3.3) and (3.4) for the last inequality.

Similarly, taking $\mathbf{q}_1$ to be the $L^2(E)$-projection of $\mathbf{q}$ onto the space of linear vectors on E, we obtain

$$|\Pi\mathbf{q}|_{2,E} = |\Pi\mathbf{q} - \mathbf{q}_1|_{2,E} \le Ch^{-2}\|\Pi\mathbf{q} - \mathbf{q}_1\|_E \\ \le Ch^{-2}(\|\Pi\mathbf{q} - \mathbf{q}\|_E + \|\mathbf{q} - \mathbf{q}_1\|_E) \le C\|\mathbf{q}\|_{2,E}.$$

The bound $\|\Pi\mathbf{q}\|_E \le C\|\mathbf{q}\|_{1,E}$ follows from the approximation property (3.4). This completes the proof of (3.8). The proof of (3.9) is similar. ∎

The following two lemmas will also be used in the analysis.

LEMMA 3.2. *If E is an h^2-parallelogram, then there exists a constant C independent of h such that*

$$(3.11) \qquad |\mathcal{K}^{-1}|_{j,\infty,\hat{E}} \le Ch^j\|K^{-1}\|_{j,\infty,E}, \quad j = 1, 2.$$

Proof. Using (3.2), we have

$$|\mathcal{K}^{-1}|_{1,\infty,\hat{E}} \le C(|\hat{K}^{-1}|_{1,\infty,\hat{E}} + h\|\hat{K}^{-1}\|_{0,\infty,\hat{E}}) \le Ch\|K^{-1}\|_{1,\infty,E},$$

where the last inequality follows from the use of the chain rule and (2.14). Similarly,

$$|\mathcal{K}^{-1}|_{2,\infty,\hat{E}} \le C(|\hat{K}^{-1}|_{2,\infty,\hat{E}} + h|\hat{K}^{-1}|_{1,\infty,\hat{E}} + h^2\|\hat{K}^{-1}\|_{0,\infty,\hat{E}}) \le Ch^2\|K^{-1}\|_{2,\infty,E},$$

where we have also used $|DF_E|_{2,\infty,\hat{E}} = 0$. ∎

Let $W^\alpha_{\mathcal{T}_h}$ consist of functions φ such that $\varphi|_E \in W^\alpha(E)$ for all $E \in \mathcal{T}_h$ and $\|\varphi\|_{\alpha,E}$ is uniformly bounded, independently of h. Let $|||\varphi|||_\alpha = \max_{E\in\mathcal{T}_h}\|\varphi\|_{\alpha,E}$.

LEMMA 3.3. *On h^2-parallelograms, if $K^{-1} \in W^{1,\infty}_{\mathcal{T}_h}$, then there exists a constant C independent of h such that for all $\mathbf{v} \in \mathbf{V}_h$*

$$(3.12) \qquad |(K^{-1}\Pi\mathbf{u}, \mathbf{v} - \Pi_0\mathbf{v})_Q| \le Ch\|\mathbf{u}\|_1\|\mathbf{v}\|.$$

Proof. On any element E we have

$$(3.13) \qquad (K^{-1}\Pi\mathbf{u}, \mathbf{v} - \Pi_0\mathbf{v})_{Q,E} = (\mathcal{K}^{-1}\hat{\Pi}\hat{\mathbf{u}}, \hat{\mathbf{v}} - \hat{\Pi}_0\hat{\mathbf{v}})_{\hat{Q},\hat{E}} \\ = ((\mathcal{K}^{-1} - \overline{\mathcal{K}^{-1}})\hat{\Pi}\hat{\mathbf{u}}, \hat{\mathbf{v}} - \hat{\Pi}_0\hat{\mathbf{v}})_{\hat{Q},\hat{E}} + (\overline{\mathcal{K}^{-1}}\hat{\Pi}\hat{\mathbf{u}}, \hat{\mathbf{v}} - \hat{\Pi}_0\hat{\mathbf{v}})_{\hat{Q},\hat{E}},$$

where $\overline{\mathcal{K}^{-1}}$ is the mean value of $\mathcal{K}^{-1}$ on $\hat{E}$. Using Taylor expansion and (2.45), we have for the first term on the right above

$$(3.14) \qquad |((\mathcal{K}^{-1} - \overline{\mathcal{K}^{-1}})\hat{\Pi}\hat{\mathbf{u}}, \hat{\mathbf{v}} - \hat{\Pi}_0\hat{\mathbf{v}})_{\hat{Q},\hat{E}}| \le C|\mathcal{K}^{-1}|_{1,\infty,\hat{E}}\|\hat{\Pi}\hat{\mathbf{u}}\|_{\hat{E}}\|\hat{\mathbf{v}}\|_{\hat{E}} \\ \le Ch\|K^{-1}\|_{1,\infty,E}\|\mathbf{u}\|_{1,E}\|\mathbf{v}\|_E,$$

where we have used (3.11), (2.43), and (3.8) for the last inequality. Using (2.40) and letting $\overline{\hat{\Pi}\hat{\mathbf{u}}}$ be the L^2-projection of $\hat{\Pi}\hat{\mathbf{u}}$ onto the space of constant vectors on $\hat{E}$, we bound the last term in (3.13) as follows:

$$\begin{aligned} |(\overline{\mathcal{K}^{-1}}\hat{\Pi}\hat{\mathbf{u}}, \hat{\mathbf{v}} - \hat{\Pi}_0\hat{\mathbf{v}})_{\hat{Q},\hat{E}}| &= |(\overline{\mathcal{K}^{-1}}(\hat{\Pi}\hat{\mathbf{u}} - \overline{\hat{\Pi}\hat{\mathbf{u}}}), \hat{\mathbf{v}} - \hat{\Pi}_0\hat{\mathbf{v}})_{\hat{Q},\hat{E}}| \\ &\le C\|\mathcal{K}^{-1}\|_{0,\infty,\hat{E}}|\hat{\Pi}\hat{\mathbf{u}}|_{1,\hat{E}}\|\hat{\mathbf{v}}\|_{\hat{E}} \le Ch\|K^{-1}\|_{0,\infty,E}\|\mathbf{u}\|_{1,E}\|\mathbf{v}\|_E, \end{aligned} \tag{3.15}$$

where we have also used (2.32), (3.7), and (3.8). The proof is completed by combining (3.13)–(3.15). □

3.1. First-order convergence for the velocity. Subtracting the numerical method (2.41)–(2.42) from the variational formulation (2.6)–(2.7), we obtain the error equations

$$\begin{aligned} (K^{-1}(\Pi\mathbf{u} - \mathbf{u}_h), \mathbf{v})_Q = (Q_h p - p_h, \nabla\cdot\mathbf{v}) \\ - (K^{-1}\mathbf{u}, \mathbf{v}) + (K^{-1}\Pi\mathbf{u}, \mathbf{v})_Q, \quad \mathbf{v} \in \mathbf{V}_h, \end{aligned} \tag{3.16}$$

$$(\nabla\cdot(\Pi\mathbf{u} - \mathbf{u}_h), w) = 0, \quad w \in W_h. \tag{3.17}$$

The last two terms in (3.16) can be manipulated as follows:

$$\begin{aligned} &- (K^{-1}\mathbf{u}, \mathbf{v}) + (K^{-1}\Pi\mathbf{u}, \mathbf{v})_Q = -(K^{-1}\mathbf{u}, \mathbf{v} - \Pi_0\mathbf{v}) - (K^{-1}(\mathbf{u} - \Pi\mathbf{u}), \Pi_0\mathbf{v}) \\ &\quad - (K^{-1}\Pi\mathbf{u}, \Pi_0\mathbf{v}) + (K^{-1}\Pi\mathbf{u}, \Pi_0\mathbf{v})_Q + (K^{-1}\Pi\mathbf{u}, \mathbf{v} - \Pi_0\mathbf{v})_Q. \end{aligned} \tag{3.18}$$

For the first term on the right above we have

$$(K^{-1}\mathbf{u}, \mathbf{v} - \Pi_0\mathbf{v}) = 0, \tag{3.19}$$

which follows by taking $\mathbf{v} - \Pi_0\mathbf{v}$ as a test function in the variational formulation (2.6) and using (2.27). Using (3.4) and (2.28), the second term on the right in (3.18) can be bounded as

$$|(K^{-1}(\mathbf{u} - \Pi\mathbf{u}), \Pi_0\mathbf{v})| \le Ch\|K^{-1}\|_{0,\infty}\|\mathbf{u}\|_1\|\mathbf{v}\|. \tag{3.20}$$

The third and fourth term on the right in (3.18) represent the quadrature error, which can be bounded by Lemma 3.5 as

$$|\sigma(K^{-1}\Pi\mathbf{u}, \Pi_0\mathbf{v})| \le Ch|\!|\!|K^{-1}|\!|\!|_{1,\infty}\|\mathbf{u}\|_1\|\mathbf{v}\|, \tag{3.21}$$

using also (3.8) and (2.28). The last term on the right in (3.18) is bounded in Lemma 3.3.

We take $\mathbf{v} = \Pi\mathbf{u} - \mathbf{u}_h$ in the error equation (3.16) above. Note that

$$\nabla\cdot(\Pi\mathbf{u} - \mathbf{u}_h) = 0, \tag{3.22}$$

since, due to (2.19), we can choose $w = J_E\nabla\cdot(\Pi\mathbf{u} - \mathbf{u}_h) \in W_h$ on any element E in (3.17) and J_E is uniformly positive. Combining (3.18)–(3.21) with (2.44) and (3.12), we obtain

$$\|\Pi\mathbf{u} - \mathbf{u}_h\| \le Ch|\!|\!|K^{-1}|\!|\!|_{1,\infty}\|\mathbf{u}\|_1. \tag{3.23}$$

The theorem below now follows from (3.23), (3.22), (3.4), and (3.6).

THEOREM 3.4. *If $K^{-1} \in W^{1,\infty}_{\mathcal{T}_h}$, then, for the velocity $\mathbf{u}_h$ of the MFMFE method* (2.41)–(2.42), *there exists a constant C independent of h such that*

$$\|\mathbf{u} - \mathbf{u}_h\| \le Ch\|\mathbf{u}\|_1, \tag{3.24}$$

$$\|\nabla \cdot (\mathbf{u} - \mathbf{u}_h)\| \le Ch\|\nabla \cdot \mathbf{u}\|_1. \tag{3.25}$$

We now proceed with the analysis of the quadrature error.

LEMMA 3.5. *If $K^{-1} \in W^{1,\infty}_{\mathcal{T}_h}$, then there exists a constant C independent of h such that for all $\mathbf{q} \in \mathbf{V}_h$ and for all $\mathbf{v} \in \mathbf{V}_h^0$,*

$$|\sigma(K^{-1}\mathbf{q}, \mathbf{v})| \le C \sum_{E \in \mathcal{T}_h} h\|K^{-1}\|_{1,\infty,E}\|\mathbf{q}\|_{1,E}\|\mathbf{v}\|_E. \tag{3.26}$$

Proof. We first consider the case of simplicial elements. We have on any element E

$$|\sigma_E(K^{-1}\mathbf{q}, \mathbf{v})| \le |\sigma_E((K^{-1} - \overline{K^{-1}})\mathbf{q}, \mathbf{v})| + |\sigma_E(\overline{K^{-1}}\mathbf{q}, \mathbf{v})|, \tag{3.27}$$

where $\overline{K^{-1}}$ is the mean value of K^{-1} on E. For the first term on the right we have

$$|\sigma_E((K^{-1} - \overline{K^{-1}})\mathbf{q}, \mathbf{v})| \le Ch|K^{-1}|_{1,\infty,E}\|\mathbf{q}\|_E\|\mathbf{v}\|_E, \tag{3.28}$$

where we have used Taylor expansion and (2.45). Let $\overline{\mathbf{q}}$ be the L^2-projection of $\mathbf{q}$ onto the space of constant vectors on E. For the second term on the right in (3.27), using Lemma 2.1, we have that

$$|\sigma_E(\overline{K^{-1}}\mathbf{q}, \mathbf{v})| = |\sigma_E(\overline{K^{-1}}(\mathbf{q} - \overline{\mathbf{q}}), \mathbf{v})| \le Ch\|K^{-1}\|_{0,\infty,E}\|\mathbf{q}\|_{1,E}\|\mathbf{v}\|_E, \tag{3.29}$$

using (3.3). Combining (3.27)–(3.29), we obtain

$$|\sigma_E(K^{-1}\mathbf{q}, \mathbf{v})| \le Ch\|K^{-1}\|_{1,\infty,E}\|\mathbf{q}\|_{1,E}\|\mathbf{v}\|_E, \tag{3.30}$$

completing the proof of (3.26) for simplicial elements.

Next, consider the quadrature error on h^2-parallelograms. We have

$$\sigma_E(K^{-1}\mathbf{q}, \mathbf{v}) = \hat{\sigma}_{\hat{E}}(\mathcal{K}^{-1}\hat{\mathbf{q}}, \hat{\mathbf{v}}) = \hat{\sigma}_{\hat{E}}((\mathcal{K}^{-1} - \overline{\mathcal{K}^{-1}})\hat{\mathbf{q}}, \hat{\mathbf{v}}) + \hat{\sigma}_{\hat{E}}(\overline{\mathcal{K}^{-1}}\hat{\mathbf{q}}, \hat{\mathbf{v}}), \tag{3.31}$$

where $\overline{\mathcal{K}^{-1}}$ is the mean value of $\mathcal{K}^{-1}$ on $\hat{E}$. Using Taylor expansion, the first term on the right above can be bounded as

$$|\hat{\sigma}_{\hat{E}}((\mathcal{K}^{-1} - \overline{\mathcal{K}^{-1}})\hat{\mathbf{q}}, \hat{\mathbf{v}})| \le C|\mathcal{K}^{-1}|_{1,\infty,\hat{E}}\|\hat{\mathbf{q}}\|_{\hat{E}}\|\hat{\mathbf{v}}\|_{\hat{E}} \le Ch\|K^{-1}\|_{1,\infty,E}\|\mathbf{q}\|_E\|\mathbf{v}\|_E, \tag{3.32}$$

where we used (3.11) and (2.43) for the last inequality. For the last term in (3.31) we have that $\hat{\sigma}_{\hat{E}}(\overline{\mathcal{K}^{-1}}\hat{\mathbf{q}}_0, \hat{\mathbf{v}}) = 0$ for any constant vector $\hat{\mathbf{q}}_0$, since the trapezoidal quadrature rule $(\cdot,\cdot)_{\hat{Q},\hat{E}}$ is exact for linear functions. Hence, the Bramble–Hilbert lemma [13] implies

$$|\hat{\sigma}_{\hat{E}}(\overline{\mathcal{K}^{-1}}\hat{\mathbf{q}}, \hat{\mathbf{v}})| \le C\|\mathcal{K}^{-1}\|_{0,\infty,\hat{E}}|\hat{\mathbf{q}}|_{1,\hat{E}}\|\hat{\mathbf{v}}\|_{\hat{E}}.$$

Using (3.7) and (2.32), we obtain

$$|\hat{\sigma}_{\hat{E}}(\overline{\mathcal{K}^{-1}}\hat{\mathbf{q}}, \hat{\mathbf{v}})| \le Ch\|K^{-1}\|_{0,\infty,E}\|\mathbf{q}\|_{1,E}\|\mathbf{v}\|_E. \tag{3.33}$$

The above bound, together with (3.31)–(3.32), implies that

$$|\sigma_E(K^{-1}\mathbf{q}, \mathbf{v})| \le Ch\|K^{-1}\|_{1,\infty,E}\|\mathbf{q}\|_{1,E}\|\mathbf{v}\|_E.$$

The proof is completed by summing over all elements E. ∎

4. Error estimates for the pressure. In this section we use a standard inf-sup argument to prove optimal convergence for the pressure. We also employ a duality argument to establish superconvergence for the pressure at the element centers of mass.

4.1. First-order convergence for the pressure. We start with an optimal error bound for the pressure.

THEOREM 4.1. *If $K^{-1} \in W^{1,\infty}_{\mathcal{T}_h}$, then, for the pressure p_h of the MFMFE method* (2.41)–(2.42)*, there exists a constant C independent of h such that*

$$\|p - p_h\| \le Ch(\|\mathbf{u}\|_1 + \|p\|_1).$$

Proof. It is well known [27, 15, 32] that the RT_0 spaces $\mathbf{V}_h^0 \times W_h^0$ satisfy the inf-sup condition

$$\inf_{0\ne w\in W_h^0}\sup_{0\ne\mathbf{v}\in\mathbf{V}_h^0}\frac{(\nabla\cdot\mathbf{v}, w)}{\|\mathbf{v}\|_{\mathrm{div}}\|w\|} \ge \beta, \tag{4.1}$$

where β is a positive constant independent of h. Using (4.1) and (3.16), we obtain

$$\begin{aligned}
&\|\mathcal{Q}_h p - p_h\| \\
&\quad\le \frac{1}{\beta}\sup_{0\ne\mathbf{v}\in\mathbf{V}_h^0}\frac{(\nabla\cdot\mathbf{v}, \mathcal{Q}_h p - p_h)}{\|\mathbf{v}\|_{\mathrm{div}}} \\
&\quad= \frac{1}{\beta}\sup_{0\ne\mathbf{v}\in\mathbf{V}_h^0}\frac{(K^{-1}(\Pi\mathbf{u}-\mathbf{u}_h), \mathbf{v})_Q - (K^{-1}(\Pi\mathbf{u}-\mathbf{u}), \mathbf{v}) + \sigma(K^{-1}\Pi\mathbf{u}, \mathbf{v})}{\|\mathbf{v}\|_{\mathrm{div}}} \\
&\quad\le \frac{C}{\beta}h\|K^{-1}\|_{1,\infty}\|\mathbf{u}\|_1,
\end{aligned}$$

where we have used the Cauchy–Schwarz inequality, (3.23), and (3.26) in the last inequality. The proof is completed by an application of the triangle inequality and (3.3). ∎

4.2. Second-order convergence for the pressure. We continue with the superconvergence estimate. We first present a bound on the quadrature error that will be used in the analysis.

LEMMA 4.2. *Let $K^{-1} \in W^{2,\infty}_{\mathcal{T}_h}$. On simplicial elements, for all $\mathbf{v}, \mathbf{q} \in \mathbf{V}_h$, there exists a positive constant C independent of h such that*

$$|\sigma(K^{-1}\mathbf{q}, \mathbf{v})| \le C\sum_{E\in\mathcal{T}_h} h^2\|K^{-1}\|_{2,\infty,E}\|\mathbf{q}\|_{1,E}\|\mathbf{v}\|_{1,E}. \tag{4.2}$$

On h^2-parallelograms, for all $\mathbf{q} \in \mathbf{V}_h$, $\mathbf{v} \in \mathbf{V}_h^0$, there exists a positive constant C independent of h such that

$$|\sigma(K^{-1}\mathbf{q}, \mathbf{v})| \le C \sum_{E \in \mathcal{T}_h} h^2 \|K^{-1}\|_{2,\infty,E} \|\mathbf{q}\|_{2,E} \|\mathbf{v}\|_{1,E}. \tag{4.3}$$

Proof. We present first the proof for simplicial elements. For any element E, using Lemma 2.1, we have

$$\begin{aligned}\sigma_E(K^{-1}\mathbf{q}, \mathbf{v}) &= \sigma_E((K^{-1} - \overline{K^{-1}})(\mathbf{q} - \bar{\mathbf{q}}), \mathbf{v}) + \sigma_E((K^{-1} - \overline{K^{-1}})\bar{\mathbf{q}}, \mathbf{v} - \bar{\mathbf{v}}) \\ &\quad + \sigma_E(K^{-1}\bar{\mathbf{q}}, \bar{\mathbf{v}}) + \sigma_E(\overline{K^{-1}}(\mathbf{q} - \bar{\mathbf{q}}), \mathbf{v} - \bar{\mathbf{v}}),\end{aligned} \tag{4.4}$$

where $\bar{\mathbf{q}}$ and $\bar{\mathbf{v}}$ are the $L^2(E)$-orthogonal projections of $\mathbf{q}$ and $\mathbf{v}$, respectively, onto the space of constant vectors, and $\overline{K^{-1}}$ is the mean value of K^{-1} on E. Using (2.45), the first, second, and fourth term on the right above are bounded by

$$Ch^2 \|K^{-1}\|_{1,\infty,E} \|\mathbf{q}\|_{1,E} \|\mathbf{v}\|_{1,E}. \tag{4.5}$$

For the third term on the right in (4.4) it is easy to check that the quadrature rule is exact for linear tensors. An application of the Bramble–Hilbert lemma [13] gives

$$|\sigma_E(K^{-1}\bar{\mathbf{q}}, \bar{\mathbf{v}})| \le Ch^2 |K^{-1}\bar{\mathbf{q}}|_{2,E} \|\bar{\mathbf{v}}\|_E \le Ch^2 |K^{-1}|_{2,\infty,E} \|\mathbf{q}\|_E \|\mathbf{v}\|_E. \tag{4.6}$$

A combination of (4.4)–(4.6) completes the proof for simplicial elements.

We proceed with the bound on the quadrature error in the case of h^2-parallelograms. We have

$$\sigma_E(K^{-1}\mathbf{q}, \mathbf{v}) = \hat{\sigma}_{\hat{E}}(\mathcal{K}^{-1}\hat{\mathbf{q}}, \hat{\mathbf{v}}) = \hat{\sigma}_{\hat{E}}((\mathcal{K}^{-1}\hat{\mathbf{q}})_1, \hat{v}_1) + \hat{\sigma}_{\hat{E}}((\mathcal{K}^{-1}\hat{\mathbf{q}})_2, \hat{v}_2). \tag{4.7}$$

Let us consider the first term on the right. Since the quadrature rule is exact for linear functions, the Peano kernel theorem [31, Theorem 5.2–3] implies

$$\begin{aligned}\hat{\sigma}_{\hat{E}}((\mathcal{K}^{-1}\hat{\mathbf{q}})_1, \hat{v}_1) &= \int_0^1 \int_0^1 \varphi(\hat{x}) \frac{\partial^2}{\partial \hat{x}^2}((\mathcal{K}^{-1}\hat{\mathbf{q}})_1 \hat{v}_1)(\hat{x}, 0) d\hat{x}\, d\hat{y} \\ &\quad + \int_0^1 \int_0^1 \varphi(\hat{y}) \frac{\partial^2}{\partial \hat{y}^2}((\mathcal{K}^{-1}\hat{\mathbf{q}})_1 \hat{v}_1)(0, \hat{y})\, d\hat{x} d\hat{y} \\ &\quad + \int_0^1 \int_0^1 \psi(\hat{x}, \hat{y}) \frac{\partial^2}{\partial \hat{x} \partial \hat{y}}((\mathcal{K}^{-1}\hat{\mathbf{q}})_1 \hat{v}_1)(\hat{x}, \hat{y}) d\hat{x}\, d\hat{y},\end{aligned} \tag{4.8}$$

where $\varphi(s) = s(s-1)/2$ and $\psi(s,t) = (1-s)(1-t) - 1/4$. Therefore, using that $\hat{\mathbf{v}}$ is linear,

$$\begin{aligned}|\hat{\sigma}_{\hat{E}}((\mathcal{K}^{-1}\hat{\mathbf{q}})_1, \hat{v}_1)| &\le C((|\mathcal{K}^{-1}|_{1,\infty,\hat{E}} \|\hat{\mathbf{q}}\|_{\hat{E}} + \|\mathcal{K}^{-1}\|_{0,\infty,\hat{E}} |\hat{\mathbf{q}}|_{1,\hat{E}}) |\hat{\mathbf{v}}|_{1,\hat{E}} \\ &\quad + (|\mathcal{K}^{-1}|_{2,\infty,\hat{E}} \|\hat{\mathbf{q}}\|_{\hat{E}} + |\mathcal{K}^{-1}|_{1,\infty,\hat{E}} |\hat{\mathbf{q}}|_{1,\hat{E}} + \|\mathcal{K}^{-1}\|_{0,\infty,\hat{E}} |\hat{\mathbf{q}}|_{2,\hat{E}}) \|\hat{\mathbf{v}}\|_{\hat{E}}).\end{aligned}$$

The term $\hat{\sigma}_{\hat{E}}((\mathcal{K}^{-1}\hat{\mathbf{q}})_2, \hat{v}_2)$ in (4.7) can be bounded similarly. Using (4.7), (2.32), (3.11), and (3.7), we obtain

$$|\sigma_E(K^{-1}\mathbf{q}, \mathbf{v})| \le Ch^2 \|K^{-1}\|_{2,\infty,E} \|\mathbf{q}\|_{2,E} \|\mathbf{v}\|_{1,E}.$$

Summing over all elements completes the proof. ∎

We are now ready to establish superconvergence of the pressure at the cell centers.

THEOREM 4.3. *Assume that* $K \in W^{1,\infty}_{\mathcal{T}_h}$ *and* $K^{-1} \in W^{2,\infty}_{\mathcal{T}_h}$ *and the elliptic regularity* (4.11) *below holds. Then, for the pressure* p_h *of the MFMFE method* (2.41)–(2.42)*, there exists a constant* C *independent of* h *such that*

$$\|\mathcal{Q}_h p - p_h\| \le Ch^2(\|\mathbf{u}\|_1 + \|\nabla\cdot\mathbf{u}\|_1) \quad \textit{on simplices} \tag{4.9}$$

and

$$\|\mathcal{Q}_h p - p_h\| \le Ch^2\|\mathbf{u}\|_2 \quad \textit{on } h^2\textit{-parallelograms.} \tag{4.10}$$

Proof. The proof is based on a duality argument. Let ϕ be the solution of

$$\begin{aligned} -\nabla\cdot K\nabla\phi &= -(\mathcal{Q}_h p - p_h) && \text{in} \quad \Omega,\\ \phi &= 0 && \text{on} \quad \Gamma_D,\\ -K\nabla\phi\cdot\mathbf{n} &= 0 && \text{on} \quad \Gamma_N. \end{aligned}$$

We assume that this problem has H^2-elliptic regularity:

$$\|\phi\|_2 \le C\|\mathcal{Q}_h p - p_h\|_0. \tag{4.11}$$

Sufficient conditions for (4.11) can be found in [22, 26]. For example, (4.11) holds if the components of $K \in C^{0,1}(\overline{\Omega})$, $\partial\Omega$ is smooth enough, and either Γ_D or Γ_N is empty.

Let us consider first the case of simplicial elements. Here it is more convenient to rewrite the error equation (3.16) as

$$(K^{-1}(\mathbf{u}-\mathbf{u}_h),\mathbf{v}) = (Q_h p - p_h, \nabla\cdot\mathbf{v}) - \sigma(K^{-1}\mathbf{u}_h,\mathbf{v}). \tag{4.12}$$

Take $\mathbf{v} = \Pi K\nabla\phi \in \mathbf{V}_h$ in (4.12) to get

$$\begin{aligned} \|\mathcal{Q}_h p - p_h\|_0^2 &= (\mathcal{Q}_h p - p_h, \nabla\cdot\Pi K\nabla\phi)\\ &= (K^{-1}(\mathbf{u}-\mathbf{u}_h),\Pi K\nabla\phi) + \sigma(K^{-1}\mathbf{u}_h,\Pi K\nabla\phi). \end{aligned} \tag{4.13}$$

For the first term on the right above we have

$$\begin{aligned} &(K^{-1}(\mathbf{u}-\mathbf{u}_h),\Pi K\nabla\phi)\\ &\quad= (K^{-1}(\mathbf{u}-\mathbf{u}_h),\Pi K\nabla\phi - K\nabla\phi) + (\mathbf{u}-\mathbf{u}_h,\nabla\phi)\\ &\quad= (K^{-1}(\mathbf{u}-\mathbf{u}_h),\Pi K\nabla\phi - K\nabla\phi) - (\nabla\cdot(\mathbf{u}-\mathbf{u}_h),\phi - \mathcal{Q}_h\phi)\\ &\quad\le C(h\|\mathbf{u}-\mathbf{u}_h\|\|K\|_{1,\infty}\|\phi\|_2 + h\|\nabla\cdot(\mathbf{u}-\mathbf{u}_h)\|\|\phi\|_1)\\ &\quad\le Ch^2\|K\|_{1,\infty}(\|\mathbf{u}\|_1 + \|\nabla\cdot\mathbf{u}\|_1)\|\phi\|_2, \end{aligned} \tag{4.14}$$

where we have used (3.4) and (3.3) for the first inequality, and (3.24) and (3.25) for the second inequality.

Using (4.2), we bound the second term on the right in (4.13) as

$$\begin{aligned} &|\sigma(K^{-1}\mathbf{u}_h,\Pi K\nabla\phi)|\\ &\quad\le C\|K^{-1}\|_{2,\infty}\sum_{E\in\mathcal{T}_h} h^2\|\mathbf{u}_h\|_{1,E}\|\Pi K\nabla\phi\|_{1,E}\\ &\quad\le C\|K^{-1}\|_{2,\infty}\sum_{E\in\mathcal{T}_h} h^2(\|\mathbf{u}_h - \Pi\mathbf{u}\|_{1,E} + \|\Pi\mathbf{u}\|_{1,E})\|K\nabla\phi\|_{1,E}\\ &\quad\le C\|K^{-1}\|_{2,\infty}\sum_{E\in\mathcal{T}_h} h^2(h^{-1}\|\mathbf{u}_h - \Pi\mathbf{u}\|_E + \|\mathbf{u}\|_{1,E})\|K\|_{1,\infty,E}\|\phi\|_{2,E}\\ &\quad\le Ch^2\|K^{-1}\|_{2,\infty}\|K\|_{1,\infty}\|\mathbf{u}\|_1\|\phi\|_2, \end{aligned} \tag{4.15}$$

where we have used (3.8), the inverse inequality (3.10), and (3.23). Now (4.9) follows from (4.13)–(4.15) and (4.11).

For the analysis on h^2-parallelograms we rewrite the error equation (3.16) in the form

$$(K^{-1}(\Pi\mathbf{u}-\mathbf{u}_h),\mathbf{v})_Q = (Q_h p - p_h, \nabla\cdot\mathbf{v}) + (K^{-1}(\Pi\mathbf{u}-\mathbf{u}),\mathbf{v}) - \sigma(K^{-1}\Pi\mathbf{u},\mathbf{v}). \tag{4.16}$$

Take $\mathbf{v} = \Pi_0 K\nabla\phi \in \mathbf{V}_h$ in (4.16) to get

$$\begin{aligned}\|\mathcal{Q}_h p - p_h\|_0^2 &= (\mathcal{Q}_h p - p_h, \nabla\cdot\Pi_0 K\nabla\phi)\\ &= (K^{-1}(\Pi\mathbf{u}-\mathbf{u}_h),\Pi_0 K\nabla\phi)_Q - (K^{-1}(\Pi\mathbf{u}-\mathbf{u}),\Pi_0 K\nabla\phi)\\ &\quad + \sigma(K^{-1}\Pi\mathbf{u},\Pi_0 K\nabla\phi).\end{aligned} \tag{4.17}$$

Using (3.4) and (3.9), the second term on the right above can be bounded as

$$|(K^{-1}(\Pi\mathbf{u}-\mathbf{u}),\Pi_0 K\nabla\phi)| \le Ch^2\|K^{-1}\|_{0,\infty}|\!|\!|K|\!|\!|_{1,\infty}\|\mathbf{u}\|_2\|\phi\|_2. \tag{4.18}$$

For the last term on the right in (4.17), bounds (4.3), (3.8), and (3.9) imply that

$$\sigma(K^{-1}\Pi\mathbf{u},\Pi_0 K\nabla\phi) \le Ch^2|\!|\!|K^{-1}|\!|\!|_{2,\infty}|\!|\!|K|\!|\!|_{1,\infty}\|\mathbf{u}\|_2\|\phi\|_2. \tag{4.19}$$

The first term on the right in (4.17) can be manipulated as follows:

$$\begin{aligned}&(K^{-1}(\Pi\mathbf{u}-\mathbf{u}_h),\Pi_0 K\nabla\phi)_{Q,E}\\ &\quad= ((K^{-1}-K_0^{-1})(\Pi\mathbf{u}-\mathbf{u}_h),\Pi_0 K\nabla\phi)_{Q,E} + (K_0^{-1}(\Pi\mathbf{u}-\mathbf{u}_h),\Pi_0(K-K_0)\nabla\phi)_{Q,E}\\ &\qquad + (K_0^{-1}(\Pi\mathbf{u}-\mathbf{u}_h),\Pi_0 K_0(\nabla\phi-\nabla\phi_1))_{Q,E} + (K_0^{-1}(\Pi\mathbf{u}-\mathbf{u}_h),\Pi_0 K_0\nabla\phi_1)_{Q,E},\end{aligned} \tag{4.20}$$

where K_0 is the value of K at the center of E and ϕ_1 is a linear approximation to ϕ such that (see [13])

$$\|\phi-\phi_1\|_E \le Ch^2\|\phi\|_{2,E}, \quad \|\phi-\phi_1\|_{1,E} \le Ch\|\phi\|_{2,E}. \tag{4.21}$$

Using (3.9), the first term on the right in (4.20) can be bounded as

$$|((K^{-1}-K_0^{-1})(\Pi\mathbf{u}-\mathbf{u}_h),\Pi_0 K\nabla\phi)_{Q,E}| \le Ch\|K^{-1}\|_{1,\infty,E}\|K\|_{1,\infty,E}\|\Pi\mathbf{u}-\mathbf{u}_h\|_E\|\phi\|_{2,E}. \tag{4.22}$$

For the second and third terms on the right in (4.20) we use that for any $\psi \in (H^1(E))^2$

$$\|\Pi_0\psi\|_E \le \|\Pi_0\psi-\psi\|_E + \|\psi\|_E \le C(h\|\psi\|_{1,E} + \|\psi\|_E)$$

to obtain

$$|(K_0^{-1}(\Pi\mathbf{u}-\mathbf{u}_h),\Pi_0(K-K_0)\nabla\phi)_{Q,E}| \le Ch\|K^{-1}\|_{0,\infty,E}\|K\|_{1,\infty,E}\|\Pi\mathbf{u}-\mathbf{u}_h\|_E\|\phi\|_{2,E} \tag{4.23}$$

and

$$\begin{aligned}&|(K_0^{-1}(\Pi\mathbf{u}-\mathbf{u}_h),\Pi_0 K_0(\nabla\phi-\nabla\phi_1))_{Q,E}|\\ &\qquad \le Ch\|K^{-1}\|_{0,\infty,E}\|K\|_{0,\infty,E}\|\Pi\mathbf{u}-\mathbf{u}_h\|_E\|\phi\|_{2,E},\end{aligned} \tag{4.24}$$

having also used (4.21) in the last inequality. For the last term in (4.20) we have

$$(K_0^{-1}(\Pi\mathbf{u}-\mathbf{u}_h),\Pi_0 K_0\nabla\phi_1)_{Q,E} = (\Pi\mathbf{u}-\mathbf{u}_h,\nabla\phi_1)_{Q,E} = (\hat\Pi\hat{\mathbf{u}}-\hat{\mathbf{u}}_h,\hat\nabla\hat\phi_1)_{\hat Q,\hat E}, \tag{4.25}$$

using $\nabla\phi_1 = (DF^{-1})^T\hat\nabla\hat\phi_1$ in the second equality. Note that $\hat\phi(\hat x,\hat y)$ is a bilinear function. Let $\tilde\phi_1$ be the linear part of $\hat\phi_1$. We have

$$(\hat\Pi\hat{\mathbf{u}}-\hat{\mathbf{u}}_h,\hat\nabla\hat\phi_1)_{\hat Q,\hat E} = (\hat\Pi\hat{\mathbf{u}}-\hat{\mathbf{u}}_h,\hat\nabla(\hat\phi_1-\tilde\phi_1))_{\hat Q,\hat E} + (\hat\Pi\hat{\mathbf{u}}-\hat{\mathbf{u}}_h,\hat\nabla\tilde\phi_1)_{\hat Q,\hat E}. \tag{4.26}$$

Since (see (2.8))

$$\hat\nabla(\hat\phi_1-\tilde\phi_1) = [(\mathbf{r}_{34}-\mathbf{r}_{21})\cdot\nabla\phi_1]\begin{pmatrix}\hat y\\ \hat x\end{pmatrix},$$

(3.1) implies

$$\begin{aligned}|(\hat\Pi\hat{\mathbf{u}}-\hat{\mathbf{u}}_h,\hat\nabla(\hat\phi_1-\tilde\phi_1))_{\hat Q,\hat E}| &\le Ch^2\|\hat\Pi\hat{\mathbf{u}}-\hat{\mathbf{u}}_h\|_{\hat E}\|\nabla\phi_1\|_{\hat E}\\ &\le Ch\|\Pi\mathbf{u}-\mathbf{u}_h\|_E\|\nabla\phi_1\|_E \le Ch\|\Pi\mathbf{u}-\mathbf{u}_h\|_E\|\phi\|_{2,E}.\end{aligned} \tag{4.27}$$

It remains to bound the last term in (4.26). Using (2.40) and the fact that the trapezoidal rule is exact for linear functions, we have

$$\begin{aligned}(\hat\Pi\hat{\mathbf{u}}-\hat{\mathbf{u}}_h,\hat\nabla\tilde\phi_1)_{\hat Q,\hat E} &= (\hat\Pi_0(\hat\Pi\hat{\mathbf{u}}-\hat{\mathbf{u}}_h),\hat\nabla\tilde\phi_1)_{\hat Q,\hat E} = (\hat\Pi_0(\hat\Pi\hat{\mathbf{u}}-\hat{\mathbf{u}}_h),\hat\nabla\tilde\phi_1)_{\hat E}\\ &= (\hat\Pi_0(\hat\Pi\hat{\mathbf{u}}-\hat{\mathbf{u}}_h),\hat\nabla(\tilde\phi_1-\hat\phi_1))_{\hat E} + (\hat\Pi_0(\hat\Pi\hat{\mathbf{u}}-\hat{\mathbf{u}}_h),\hat\nabla\hat\phi_1)_{\hat E}.\end{aligned} \tag{4.28}$$

The first term on the right in (4.28) is bounded similarly to (4.27):

$$|(\hat\Pi_0(\hat\Pi\hat{\mathbf{u}}-\hat{\mathbf{u}}_h),\hat\nabla(\tilde\phi_1-\hat\phi_1))_{\hat E}| \le Ch\|\Pi\mathbf{u}-\mathbf{u}_h\|_E\|\phi\|_{2,E}. \tag{4.29}$$

For the last term in (4.28) we have

$$(\hat\Pi_0(\hat\Pi\hat{\mathbf{u}}-\hat{\mathbf{u}}_h),\hat\nabla\hat\phi_1)_{\hat E} = (\Pi_0(\Pi\mathbf{u}-\mathbf{u}_h),\nabla\phi_1)_E. \tag{4.30}$$

Combining (4.20)–(4.30) and summing over all elements, we obtain

$$(K^{-1}(\Pi\mathbf{u}-\mathbf{u}_h),\Pi_0 K\nabla\phi)_Q = R + \sum_{E\in\mathcal{T}_h}(\Pi_0(\Pi\mathbf{u}-\mathbf{u}_h),\nabla\phi_1)_E, \tag{4.31}$$

where

$$|R| \le Ch^2|\!|\!|K^{-1}|\!|\!|_{1,\infty}|\!|\!|K|\!|\!|_{1,\infty}\|\mathbf{u}\|_1\|\phi\|_2, \tag{4.32}$$

having also used (3.23). For the last term in (4.31), using the regularity of ϕ, (3.22), (2.27), and that $(\Pi\mathbf{u}-\mathbf{u}_h)\cdot\mathbf{n}=0$ on Γ_N and $\phi=0$ on Γ_D, we obtain

$$\begin{aligned}&\left|\sum_{E\in\mathcal{T}_h}(\Pi_0(\Pi\mathbf{u}-\mathbf{u}_h),\nabla\phi_1)_E\right| = \left|\sum_{E\in\mathcal{T}_h}(\Pi_0(\Pi\mathbf{u}-\mathbf{u}_h),\nabla(\phi_1-\phi))_E\right|\\ &\quad\le C\sum_{E\in\mathcal{T}_h}\|\Pi\mathbf{u}-\mathbf{u}_h\|_E\|\phi_1-\phi\|_{1,E}\\ &\quad\le Ch^2|\!|\!|K^{-1}|\!|\!|_{1,\infty}\|\mathbf{u}\|_1\|\phi\|_2,\end{aligned} \tag{4.33}$$

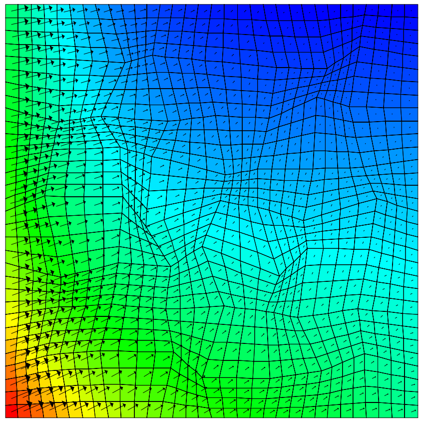

FIG. 5.1. *Computed solution on the second level of refinement in Example* 1.

where we have used (3.23) and (4.21). The proof of (4.10) is completed by combining (4.17)–(4.19) and (4.31)–(4.33), and using (4.11). □

Remark 4.1. Since $\mathcal{Q}_h p$ is $O(h^2)$-close to p at the center of mass of each element, the above theorem implies that

$$|||p - p_h||| \leq Ch^2,$$

where $|||\cdot||| = \left(\sum_E |E|(p(m_E) - p_h)^2\right)^{1/2}$ and m_E is the center of mass of E.

5. Numerical experiments. In this section we present several numerical results on quadrilateral grids that confirm the theoretical results from the previous sections.

In the first example we test the method on a sequence of meshes obtained by a uniform refinement of an initial rough quadrilateral mesh. The boundary conditions are of Dirichlet type. The tensor coefficient and the true solution are

$$K = \begin{pmatrix} 5 & 1 \\ 1 & 2 \end{pmatrix}, \quad p(x,y) = (1-x)^4 + (1-y)^3(1-x) + \sin(1-y)\cos(1-x).$$

The initial 8×8 mesh is generated from a square mesh by randomly perturbing the location of each vertex within a disk centered at the vertex with a radius $h\sqrt{2}/3$. Due to (2.31), the nonsmoothness of the grid translates into a discontinuous computational permeability $\mathcal{K}$. The computed solution on the second level of refinement is shown in Figure 5.1. The colors represent the pressure values and the arrows represent the velocity vectors. The numerical errors and asymptotic convergence rates are obtained on a sequence of six mesh refinements and are reported in Table 5.1. Here, for scalar functions $|||w|||$ is the discrete L^2-norm defined in Remark 4.1 and for vectors $|||\mathbf{v}|||$ denotes a discrete vector L^2-norm that involves only the normal vector components at the midpoints of the edges. We note that the obtained convergence rates of $O(h^2)$ for $|||p-p_h|||$ and $O(h)$ for $\|\mathbf{u}-\mathbf{u}_h\|$ confirm the theoretical results. The $O(h^2)$ accuracy for $|||\mathbf{u} - \mathbf{u}_h|||$ and $|||\nabla \cdot (\mathbf{u} - \mathbf{u}_h)|||$ indicates superconvergence for the normal velocities at the midpoints of the edges and for the divergence at the cell-centers.

In the second example we consider an irregularly shaped domain consisting of two subdomains; see Figure 5.2. The grid is nonsmooth across the interface leading

Table 5.1
Discretization errors and convergence rates for Example 1.

$1/h$	$\|\|\|p - p_h\|\|\|$	$\|\|\mathbf{u} - \mathbf{u}_h\|\|$	$\|\|\|\mathbf{u} - \mathbf{u}_h\|\|\|$	$\|\|\|\nabla \cdot (\mathbf{u} - \mathbf{u}_h)\|\|\|$
8	0.123E-1	0.882E-1	0.281E-1	0.112E-1
16	0.372E-2	0.542E-1	0.129E-1	0.287E-2
32	0.103E-2	0.292E-1	0.411E-2	0.722E-3
64	0.270E-3	0.151E-1	0.114E-2	0.181E-3
128	0.692E-4	0.772E-2	0.307E-3	0.455E-4
256	0.175E-4	0.390E-2	0.817E-4	0.127E-4
Rate	1.98	0.99	1.91	1.84

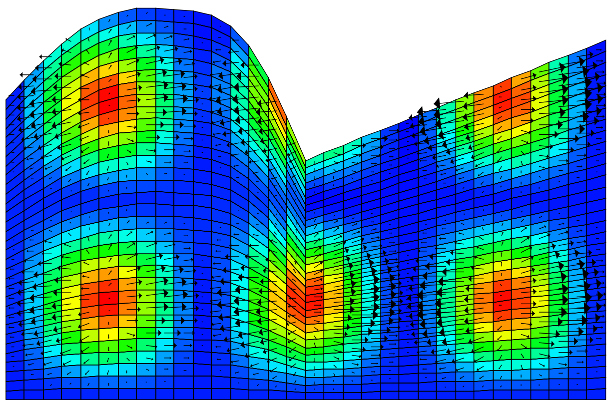

Fig. 5.2. *Computed solution on the second level of refinement in Example 2.*

to a discontinuous computational permeability $\mathcal{K}$. The permeability tensor and true solution are

$$K = \begin{pmatrix} 4 + (x+2)^2 + y^2 & 1 + \sin(xy) \\ 1 + \sin(xy) & 2 \end{pmatrix}, \quad p(x,y) = (\sin(3\pi x))^2(\sin(3\pi y))^2.$$

The boundary conditions are of Neumann type. The computed solution on the second refinement level is shown in Figure 5.2. The numerical errors and asymptotic convergence rates are presented in Table 5.2. As in the previous example, the numerical convergence rates confirm the theory.

6. Conclusions. We have presented a BDM_1-based MFE method with quadrature that reduces to CCFD for the pressure on simplicial and quadrilateral grids. The resulting algebraic system is symmetric and positive definite. The method is closely related to the MPFA method and it performs well on irregular grids and rough coefficients. The analysis is based on combining MFE techniques with quadrature error estimates. First order convergence is obtained for the pressure and the velocity in their natural norms. Second order convergence is obtained for the pressure and the element centers of mass. Computational results also indicate superconvergence for the velocity at the midpoints of the edges on h^2-parallelogram grids. We have also developed and analyzed the method on hexahedral elements that are $O(h^2)$-perturbations of parallelepipeds. These results will be presented in a forthcoming paper.

Remark 6.1. We recently learned of the concurrent and related work of Klausen and Winther [25]. They formulate the MPFA method from [1] as a MFE method

TABLE 5.2
Discretization errors and convergence rates for Example 2.

$1/h$	$\|\|\|p - p_h\|\|\|$	$\|\|\mathbf{u} - \mathbf{u}_h\|\|$	$\|\|\|\mathbf{u} - \mathbf{u}_h\|\|\|$	$\|\|\|\nabla \cdot (\mathbf{u} - \mathbf{u}_h)\|\|\|$
8	0.177E+2	0.492E0	0.512E0	0.764E-2
16	0.151E0	0.179E0	0.138E0	0.647E-4
32	0.653E-1	0.919E-1	0.513E-1	0.279E-4
64	0.185E-1	0.453E-1	0.132E-1	0.790E-5
128	0.460E-2	0.226E-1	0.334E-2	0.196E-5
256	0.116E-4	0.113E-1	0.838E-3	0.494E-6
Rate	1.99	0.99	1.99	1.99

using an enhanced Raviart–Thomas space and obtain convergence results on h^2-parallelogram grids.

REFERENCES

[1] I. Aavatsmark, *An introduction to multipoint flux approximations for quadrilateral grids*, Comput. Geosci., 6 (2002), pp. 405–432.

[2] I. Aavatsmark, T. Barkve, Ø. Bøe, and T. Mannseth, *Discretization on unstructured grids for inhomogeneous, anisotropic media.* I. *Derivation of the methods*, SIAM J. Sci. Comput., 19 (1998), pp. 1700–1716.

[3] I. Aavatsmark, G. Eigestad, R. Klausen, M. F. Wheeler, and I. Yotov, *Convergence of a Symmetric MPFA Method on Quadrilateral Grids*, Technical report TR-MATH 05-14, Department of Mathematics, University of Pittsburgh, Pittsburgh, PA, 2005.

[4] T. Arbogast, *Implementation of a locally conservative numerical subgrid upscaling scheme for two-phase Darcy flow*, Comput. Geosci., 6 (2002), pp. 453–481.

[5] T. Arbogast, L. C. Cowsar, M. F. Wheeler, and I. Yotov, *Mixed finite element methods on nonmatching multiblock grids*, SIAM J. Numer. Anal., 37 (2000), pp. 1295–1315.

[6] T. Arbogast, C. N. Dawson, P. T. Keenan, M. F. Wheeler, and I. Yotov, *Enhanced cell-centered finite differences for elliptic equations on general geometry*, SIAM J. Sci. Comput., 19 (1998), pp. 404–425.

[7] T. Arbogast, M. F. Wheeler, and I. Yotov, *Mixed finite elements for elliptic problems with tensor coefficients as cell-centered finite differences*, SIAM J. Numer. Anal., 34 (1997), pp. 828–852.

[8] D. N. Arnold, D. Boffi, and R. S. Falx, *Quadrilateral H(div) finite elements*, SIAM J. Numer. Anal., 42 (2005), pp. 2429–2451.

[9] D. N. Arnold and F. Brezzi, *Mixed and nonconforming finite element methods: Implementation, post-processing and error estimates*, RAIRO Modél. Math. Anal. Numér., 19 (1985), pp. 7–32.

[10] M. Berndt, K. Lipnikov, J. D. Moulton, and M. Shashkov, *Convergence of mimetic finite difference discretizations of the diffusion equation*, East-West J. Numer. Math., 9 (2001), pp. 265–284.

[11] M. Berndt, K. Lipnikov, M. Shashkov, M. F. Wheeler, and I. Yotov, *A mortar mimetic finite difference method on non-matching grids*, Numer. Math., 102 (2005), pp. 203–230.

[12] M. Berndt, K. Lipnikov, M. Shashkov, M. F. Wheeler, and I. Yotov, *Superconvergence of the velocity in mimetic finite difference methods on quadrilaterals*, SIAM J. Numer. Anal., 43 (2005), pp. 1728–1749.

[13] S. C. Brenner and L. R. Scott, *The Mathematical Theory of Finite Element Methods*, Texts Appl. Math. 15, Springer-Verlag, New York, 2002.

[14] F. Brezzi, J. Douglas, Jr., and L. D. Marini, *Two families of mixed elements for second order elliptic problems*, Numer. Math., 47 (1985), pp. 217–235.

[15] F. Brezzi and M. Fortin, *Mixed and Hybrid Finite Element Methods*, Springer Ser. Comput. Math. 15, Springer-Verlag, Berlin, 1991.

[16] Z. Cai, J. E. Jones, S. F. McCormick, and T. F. Russell, *Control-volume mixed finite element methods*, Comput. Geosci., 1 (1997), pp. 289–315 (1998).

[17] S.-H. Chou, D. Y. Kwak, and K. Y. Kim, *A general framework for constructing and analyzing mixed finite volume methods on quadrilateral grids: The overlapping covolume case*, SIAM J. Numer. Anal., 39 (2001), pp. 1170–1196.

[18] P. G. Ciarlet, *The Finite Element Method for Elliptic Problems*, North–Holland, New York, 1978.
[19] M. G. Edwards, *Unstructured, control-volume distributed, full-tensor finite-volume schemes with flow based grids*, Comput. Geosci., 6 (2002), pp. 433–452.
[20] M. G. Edwards and C. F. Rogers, *Finite volume discretization with imposed flux continuity for the general tensor pressure equation*, Comput. Geosci., 2 (1998), pp. 259–290 (1999).
[21] R. E. Ewing, M. Liu, and J. Wang, *Superconvergence of mixed finite element approximations over quadrilaterals*, SIAM J. Numer. Anal., 36 (1999), pp. 772–787.
[22] P. Grisvard, *Elliptic Problems in Nonsmooth Domains*, Monogr. Stud. Math. 24, Pitman, Boston, 1985.
[23] J. M. Hyman, M. Shashkov, and S. Steinberg, *The numerical solution of diffusion problems in strongly heterogeneous non-isotropic materials*, J. Comput. Phys., 132 (1997), pp. 130–148.
[24] R. A. Klausen and T. F. Russell, *Relationships among some locally conservative discretization methods which handle discontinuous coefficients*, Comput. Geosci., 8 (2004), pp. 341–377.
[25] R. A. Klausen and R. Winther, *Convergence of multi point flux approximations on quadrilateral grids*, Numer. Methods Partial Differential Equations, to appear.
[26] J. L. Lions and E. Magenes, *Non-homogeneous Boundary Value Problems and Applications*, Vol. 1, Springer-Verlag, New York, 1972.
[27] R. A. Raviart and J. M. Thomas, *A mixed finite element method for 2nd order elliptic problems*, in Mathematical Aspects of the Finite Element Methods, Lecture Notes in Math. 606, Springer-Verlag, Berlin, 1977, pp. 292–315.
[28] J. E. Roberts and J. M. Thomas, *Mixed and hybrid methods*, in Handbook of Numerical Analysis, Vol. II, P. Ciarlet and J. Lions, eds., North–Holland, Amsterdam, 1991, pp. 523–639.
[29] T. F. Russell and M. F. Wheeler, *Finite element and finite difference methods for continuous flows in porous media*, in The Mathematics of Reservoir Simulation, Frontiers Appl. Math. 1, R. E. Ewing, ed., SIAM, Philadelphia, 1984, pp. 35–106.
[30] T. F. Russell, M. F. Wheeler, and I. Yotov, *Superconvergence for control volume mixed finite element methods on rectangular grids*, SIAM J. Numer. Anal., to appear.
[31] A. H. Stroud, *Approximate Calculation of Multiple Integrals*, Prentice-Hall, Englewood Cliffs, NJ, 1971.
[32] J. Wang and T. P. Mathew, *Mixed finite element method over quadrilaterals*, in Conference on Advances in Numerical Methods and Applications, I. T. Dimov, B. Sendov, and P. Vassilevski, eds., World Scientific, River Edge, NJ, 1994, pp. 203–214.
[33] A. Weiser and M. F. Wheeler, *On convergence of block-centered finite differences for elliptic problems*, SIAM J. Numer. Anal., 25 (1988), pp. 351–375.
[34] M. F. Wheeler and I. Yotov, *A posteriori error estimates for the mortar mixed finite element method*, SIAM J. Numer. Anal., 43 (2005), pp. 1021–1042.